On the Performance of Cooperative Relaying Spectrum-Sharing Systems with Collaborative Distributed Beamforming

Ali Afana, Vahid Asghari, Ali Ghrayeb, and Sofiène Affes

***Abstract*—In this paper, we use joint distributed beamforming and cooperative relaying in cognitive radio relay networks in an effort to enhance the spectrum efficiency and improve the performance of the cognitive (secondary) system. In particular, we consider a spectrum sharing system where a set of potential relays are employed to help a pair of secondary users in the presence of a licensed (primary) user. Among the available relays, only the reliable ones participate in the beamforming process, where the beamformer weights are obtained based on a linear optimization method. We investigate two well-known strategies, namely, selection decode-and-forward (SDF) and amplify-and-forward (AF) relaying in conjunction with distributed optimal beamforming. However, given the complexity of the performance analysis with optimal beamforming, we use zero forcing beamforming (ZFB), and compare both approaches through simulations. In this context, for SDF, we derive expressions for the probability density function (PDF) of the received signal-to-interference noise ratio (SINR) at the relays as well as at the secondary destination. As for the AF scheme, we obtain the exact expression for the cumulative distribution function (CDF) and the moment generating function (MGF) of the equivalent end-to-end SNR at the secondary destination. For both schemes, we derive closed-form expressions for the outage probability and bit error rate (BER) over independent and identically distributed Rayleigh fading channels for binary phase shift keying (BPSK) and M-ary quadrature amplitude modulation (M-QAM) schemes. Numerical results demonstrate the efficacy of the proposed scheme in improving the outage and BER performance of the secondary system while limiting the interference to the primary system. In addition, the results show the effectiveness of the combination of the cooperative diversity and distributed beamforming in compensating for the loss in the secondary system's performance due to the primary user's co-channel interference (CCI).**

***Index Terms*—Cognitive radio, cooperative relaying, performance analysis, spectrum sharing, and zero forcing beamforming.**

Manuscript received May 29, 2013; revised September 5, October 29, and December 16, 2013, January 9, 2014. The editor coordinating the review of this paper and approving it for publication was E. Au.

This paper was made possible by NPRP grant # 09-126-2-054 from the Qatar National Research Fund (a member of Qatar Foundation). The statements made herein are solely the responsibility of the authors. An earlier version of this work was presented at IEEE SPAWC 2012 and IEEE GLOBECOM 2012.

A. Afana is with the Department of Electrical and Computer Engineering, Concordia University, Montreal, Canada (e-mail: a_afa@encs.concordia.ca).

V. Asghari and S. Affes are with the Institut National de la Researche Scientifique (INRS), University of Quebec, Montreal, QC, Canada (e-mail: {vahid, affes}@emt.inrs.ca).

A. Ghrayeb is with the Department of Electrical and Computer Engineering, Texas A&M University at Qatar (on leave from Concordia University, Montreal, Canada) (e-mail: ali.ghrayeb@qatar.tamu.edu).

I. Introduction

With the great demand for high data rate wireless applications, new dedicated spectrum bands have become a necessity. In fact, the radio spectrum suffers from inefficient utilization due to the fixed allocation of spectrum bands. Cognitive radio (CR) has emerged as a promising solution to the scarcity and the under-utilization of the spectrum [1]. This technology allows unlicensed users/secondary users (SUs) to share the same spectrum bands with the licensed ones/primary users (PUs) provided that the quality of service (QoS) of the PUs is guaranteed. In the literature, spectrum-sharing techniques are classified into three main models (overlay, underlay and interweave) according to the way the secondary system accesses the primary's spectrum [2]. In the overlay model, the secondary system helps the PUs to finish their transmission quickly to access their spectrum bands. In the interweave model, the SUs exploit the unoccupied bands of the PU when the latter is idle. In contrast to the overlay and the interweave schemes, in the underlay model, the SUs are allowed to transmit simultaneously with the PUs as long as the inflicted interference level at the PUs is below a predefined threshold called *interference temperature* [1]. To meet this limitation, SUs adjust their transmit power or make use of other degrees of freedom such as *beamforming* [3] to guarantee the QoS of the PU while enhancing their throughput.

Cooperative relaying on the other hand emerged as a powerful solution for improving the performance of single-antenna communication nodes. This is attributed to making use of intermediate relay nodes, which are used to assist transmission from the source to the destination. In [4], Laneman et al., introduced fixed relaying schemes, including amplify and forward (AF), decode and forward (DF), and selection relaying protocols that adapt according to the received signal-to-noise ratio (SNR). The relay can forward the signal selectively in order to decrease the probability of error propagation. If the received SNR at the relay is low, the message is most likely to have errors, and hence, the relay ignores the message. The authors in [5]-[7] and references therein considered threshold-based relaying strategies for cooperative communication networks in an effort to mitigate the impact of error propagation, resulting in preserving the diversity order of the system.

Two of the most common relaying protocols are selection decode-and-forward (SDF) and AF relaying [4]. In SDF, only a subset of the potential relays, which have good channels to the source, decode and retransmit the source's signal to the destination. Meanwhile, in AF, the relays simply amplify and forward the source's message to the destination. The performance of those schemes has been investigated intensively in conventional systems [4] and we adopt them in this paper as well. Recently, there have been a few articles on relaying schemes in cognitive radio networks (CRNs) where the inflicted interference at the PUs is limited by controlling the transmit power of the secondary transmitters [8]-[9]. The end-to-end performance of cooperative relaying in spectrum-sharing systems with QoS requirements was studied in [8] where the authors investigated the bit error rate (BER) and outage probability performance for DF relaying. This work considered only a single relay. The authors in [9] investigated the outage probability for a multi-relay system with best relay selection based on spectrum sharing constraints. Later, in [10], the exact outage performance of opportunistic SDF relaying in CRNs was derived subject to maximum transmit power limits. Recently, the capacity of reactive and proactive DF relaying in CRNs was investigated in [11] under peak power interference constraints. All these works considered either the received peak or average power interference constraints or both of them to limit the interference to PUs.

Other works exploited beamforming to mitigate interference to PUs [12]-[18]. In [12], an iterative alternating optimization-based algorithm was developed to obtain the optimal beamforming weights in order to maximize the worst signal to interference noise ratio in multiuser CRNs. In [13], authors presented an optimization framework for a wireless sensor network whereby, in a given route, the optimal relay selection and power allocation are performed subject to SNR constraints. In [14], convex optimization tools were used to find the sub-optimal beamformers in relay assisted CRNs. In [15], iterative optimization algorithms were developed to design the optimal weight beamformers aiming to maximize the worst signal-to-interference-plus-noise ratio (SINR) of multiple destinations. However, these algorithms and tools suffer from high computational complexity. Zero forcing beamforming (ZFB) is considered as a simple sub-optimal approach that can be practically implemented [16], [17]. In [18], a ZFB approach in a single relay with a collocated multi-antenna system was applied to improve the primary system performance in an overlay CR scenario. In their work, upper bounds for the outage and error probabilities were derived.

In this paper, we combine cooperative relaying and distributed beamforming with the objective of improving the secondary system's performance. Beamforming is done such that the received SNR at the secondary destination is maximized subject to a non-zero interference constraint (predefined threshold) at the primary receiver. This method of beamforming is general and encompasses ZFB as a special case. For tractability reasons, we apply distributed ZFB in conjunction with SDF and AF relaying in a spectrum sharing environment where the secondary source communicates with its destination in the presence of a PU. We limit the inflicted interference at the PU from both the secondary source and relays. A peak power interference constraint is imposed on the source's transmission in the broadcasting phase while a distributed ZFB is applied to null the interference to the PU in the the relaying phase. To analyze the secondary performance under the impact of the PU's co-channel interference (CCI), we derive the cumulative distribution functions (CDFs) and probability density functions (PDFs) of the received SINRs in the SDF scheme. For the AF scheme, the CDF and the moment generating function (MGF) of the end-to-end (E2E) equivalent SNR are derived. Making use of these statistics, we derive closed-form expressions for the outage probability and the BER of the proposed spectrum-sharing system and confirm the results numerically and by simulations for different values of interference temperatures Q, number of relays and PU's CCI interference values.

In addition, asymptotic analysis of both metrics is performed in order to investigate the achievable diversity order of the proposed system, and to gain some insight on the impact of key parameters on the overall performance. Two scenarios are considered: 1) when a fixed interference constraint is imposed, which leads to an error floor; and 2) when the interference threshold scales with the secondary transmit power, which leads to a diversity gain in the low secondary transmit power regime. We also compare the performance of the proposed schemes to the opportunistic SDF scheme presented in [9] and [10] for strict levels of the reflected interference at the PUs. We demonstrate that the proposed schemes outperform those in [9] and [10] for low to medium values of Q, which is the range of interest in cognitive radio networks.[1]

The rest of this paper is organized as follows. Section II describes the system model. The system performance of the SDF scheme is analyzed in Section III while the performance of the AF scheme is analyzed in Section IV. Numerical results are given in Section V. Section VI concludes the paper. Finally, Appendices are given in Section VII. Throughout this paper, the Frobenius norm of the vectors are denoted by $||\cdot||$. The Transpose and the Conjugate Transpose operations are denoted by $(\cdot)^T$ and $(\cdot)^\dagger$, respectively. $|x|$ means the magnitude of a complex number x. $\mathcal{CN} \sim (0,1)$ refers to a complex Gaussian random variable with zero-mean and unit variance. Diag($\mathbf{x}$) denotes a diagonal matrix whose diagonal elements are $\mathbf{x}$'s elements.

II. System Model and Problem Formulation

A. System Model

Consider a relay-assisted CRN shown in Fig. 1 where each SU and PU is equipped with a single antenna. Specifically, our system model consists of a secondary source (SS), a secondary destination (SD) and a set of secondary relays $R_i, \forall i = 1, 2, ..., M$. There is no direct link between the source and destination, and they communicate only via potential relays $L_s \leq M$ that relay the source's message. A primary system coexists in the same area with the secondary system. The SUs are allowed to share the same frequency spectrum with the PU as long as the interference to the PU is limited to a predefined threshold. Both systems transmit simultaneously in an underlay manner. The transmission protocol consists of two orthogonal time slots and is divided into two phases as shown in Fig. 1.

[1]Hereafter, for simplicity, we refer to our system models as SDF-ZFB for the selection DF relaying scheme with ZFB applied, and AF-ZFB for the AF relaying scheme with ZFB applied.

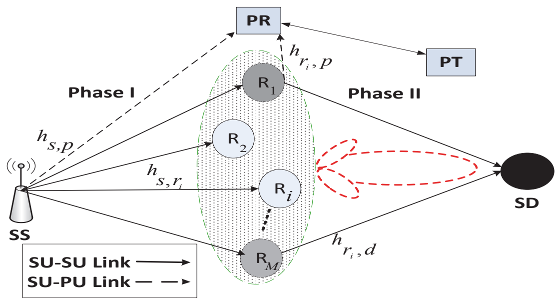

Fig. 1. System model.

In the first phase, based on the interference channel state information (CSI) between SS and PU, SS adjusts its transmit power under a predefined threshold Q and broadcasts its message to the relays. Any data transmitted from SS resulting in an interference level higher than Q, which is the maximum tolerable interference power level at PU, is not allowed. Hence, a peak power constraint is imposed on the interference received at PU. In the second phase of the SDF scheme, the potential relays, which are selected during the first-hop transmission, become members of the potential relays set $\mathcal{C}$ where ZFB is applied to null the interference from $\mathcal{C}$ to PU. Meanwhile in the AF scheme, all L_s potential relays participate in the beamforming process. By applying ZFB, the set of potential relays are able to always transmit without interfering with the PU.

B. Channel Model

All channel coefficients are assumed to be independent Rayleigh fading. Let $h_{a,b}$ denote the channel coefficient between nodes a and b, which is modeled as a zero mean, circularly symmetric complex Gaussian (CSCG) random variable with variance $\lambda_{a,b}$. n_a denotes additive white Gaussian noise which is also modeled as a zero mean, CSCG random variable with variance σ^2. Let h_{s,r_i} denote the channel coefficient between the source's transmit antenna and the receive antenna of the ith relay and $h_{r_i,d}$ represent the channel coefficient between the ith relay and SD and their channel power gains are $|h_{s,r_i}|^2$ and $|h_{r_i,d}|^2$, which are exponentially distributed with parameter λ_{s,r_i} and $\lambda_{r_i,d}$, respectively. Denote $h_{s,p}$ as the interference channel coefficient between SS and PU and its channel power gain $|h_{s,p}|^2$, which is also exponentially distributed with parameter $\lambda_{s,p}$. Let $h_{r_i,p}$, g_{m,r_i} and $g_{m,d}$ represent the interference channel coefficients between the ith relay and PU, and between the PU and both the ith relay and SD with their channel power gains $|h_{r_i,p}|^2, |g_{m,r_i}|^2$ and $|g_{m,d}|^2$ are also exponentially distributed with parameters $\lambda_{r_i,p}$, λ_{m,r_i} and $\lambda_{m,d}$, respectively. Let the ZFB vector be $\mathbf{w}_{\mathbf{zf}}^T = [w_1, w_2, ..., w_{L_s}]$. Also let $\mathbf{h}_{\mathbf{rd}}^T = [h_{r_1,d}, ..., h_{r_{L_s},d}]$, and $\mathbf{h}_{\mathbf{rp}}^T = [h_{r_1,p}, ..., h_{r_{L_s},p}]$ be the channel vectors between the relays and both SD and PU, respectively. It is assumed that SS has perfect knowledge of the interference channel between itself and the PU, i.e., h_{sp}. We also assume that each selected relay R_i has perfect knowledge about its interference channel $h_{r_i,p}$ to the PU and then it shares this channel information with the SD to design the ZFB process at the second-hop transmission. It is worth mentioning that the availability of this interference channel information can be acquired through a spectrum-band manager that mediates between the primary and secondary users [19].[2] It is also assumed that SD has perfect knowledge of the channel coefficients between the selected relays and itself, i.e., (R_i - SD), which can be obtained via traditional channel estimation [21]. In our scheme, the ZFB weights associated with the selected relays are designed at the SD by exploiting the aforementioned channel information. Then, each weight is sent back to the selected relay via a low data-rate feedback link, and that is applicable in slow fading environments [22].

C. Mathematical Model and Size of Set $\mathcal{C}$

In the underlay approach of this model, the SU can utilize the PU's spectrum as long as the interference it generates at the PUs remains below Q, which is the maximum tolerable interference level at which the PU can still maintain reliable communication [2]. Hence, the SS's power P is constrained as $P = \min\left\{\frac{Q}{|h_{s,p}|^2}, P_s\right\}$ where P_s is the maximum transmission power of SS [9]. In our model, we also assume that the PU imposes CCI at the secondary relays and SD. To this end, the received SINR $\hat{\gamma}_{s,r_i}$ at the ith relay is given as:

$$\hat{\gamma}_{s,r_i} = \min\left\{\frac{Q}{|h_{s,p}|^2}, P_s\right\} \frac{|h_{s,r_i}|^2}{P_{int}|g_{m,r_i}|^2 + \sigma^2}, \qquad (1)$$

where P_{int} is the PU's transmit power.

Lemma 1: The CDF of $\hat{\gamma}_{s,r_i}$, i.e., $F_{\hat{\gamma}_{s,r_i}}(\gamma)$ is given as

$$\begin{aligned} F_{\hat{\gamma}_{s,r_i}}(\gamma) &= 1 - F_{h_{s,p}}(\vartheta) - \frac{Q\lambda_{s,p}\lambda_{m,r_i} e^{-\lambda_{s,p}\vartheta + \frac{\lambda_{m,r_i}\sigma^2}{P_{int}}}}{\lambda_{s,r_i} P_{int}\gamma} \\ &\times \left(-e^{\frac{Q\lambda_{s,p}}{\lambda_{s,r_i}\gamma}\left(\frac{\lambda_{m,r_i}}{P_{int}} + \frac{\lambda_{s,r_i}\gamma}{Q}\right)}\right. \\ &\times \left. Ei\left[-\left(\sigma^2 + \frac{Q\lambda_{s,p}}{\gamma\lambda_{s,r_i}}\right)\left(\frac{\lambda_{m,r_i}}{P_{int}} + \frac{\lambda_{s,r_i}\gamma}{Q}\right)\right]\right) \\ &+ F_{h_{s,p}}(\vartheta)\left(1 - \frac{e^{-\frac{\sigma^2\lambda_{s,p}\gamma}{P_s}} P_s}{P_{int}\lambda_{s,p}\gamma + P_s\lambda_{m,r_i}}\right), \end{aligned} \qquad (2)$$

where $\vartheta = \frac{Q}{P_s}$, $F_{h_{s,p}}(\vartheta) = 1 - e^{-\lambda_{s,p}\vartheta}$ and $Ei[.]$ is the exponential integral defined in [28].

Proof: See Appendix A. ■

[2]We acknowledge that obtaining the interference channel between the primary and secondary users is a challenging problem in practice. However, the level of interference caused on the PU can be estimated by the fact that SS can hear the uplink signal of the PU. Feeding back the interference CSI to the SS may be carried out directly by the licensee or indirectly through a band manager, which mediates between the two parties (top of page 6 of [19]). To this end, several protocols have been proposed in [19]-[20], which allow secondary and primary users to collaborate and exchange information such that the interference channel gains can be directly fed-back from the primary receiver to the secondary network.

For AWGN only, i.e. $P_{int} = 0$, the CDF of the received SNR at the ith relay γ_{s,r_i} is given as [16]

$$F_{\gamma_{s,r_i}}(\gamma) = 1 - e^{\frac{-\lambda_{s,p}\gamma}{\gamma_s}} + \frac{\gamma e^{-\frac{\frac{\lambda_{s,r_i}Q}{\sigma^2}+\lambda_{s,p}\gamma}{\gamma_s}}}{\frac{\lambda_{s,r_i}Q}{\lambda_{s,p}}+\gamma}, \tag{3}$$

where $\gamma_s = \frac{P_s}{\sigma^2}$.

We define $\mathcal{C}$ to be the set of relays which have their received instantaneous SNRs exceeding a certain threshold in the first time slot. This translates to the fact that the mutual information between SS and each relay is above a specified target value. In this case, the potential ith relay is only required to meet the following constraint given as [4]

$$\Pr\left[R_i \in \mathcal{C}\right] = \Pr\left[\frac{1}{2}\log_2(1+\gamma^*_{s,r_i}) \geq R_{min}\right], i = 1, 2, ..., M, \tag{4}$$

where the coefficient $\frac{1}{2}$ comes from the dual-hop transmission in two time slots, γ^*_{s,r_i} represents either γ_{s,r_i} or $\hat{\gamma}_{s,r_i}$ and R_{min} denotes the minimum target rate below which outage occurs. According to (3), we can obtain

$$\Pr\left[R_i \in \mathcal{C}\right] = 1 - F_{\gamma^*_{s,r_i}}(\gamma_{min}), \tag{5}$$

where $\gamma_{min} = 2^{2R_{min}} - 1$ is the SINR threshold.

Without loss of generality, for all sub-channels being symmetrical, i.e., $\lambda_{s,r_i} = \lambda_{s,r}\,\forall\, i$, then $\Pr\left[R_i \in \mathcal{C}\right]$ is exactly the same for all i. Let $\Pr\left[R_i \in \mathcal{C}\right] = q$, and denote the cardinality of the set $\mathcal{C}$ as $|\mathcal{C}|$, then according to the Binomial Law, $\Pr\left[|\mathcal{C}| = L_s\right]$ becomes

$$\Pr\left[|\mathcal{C}| = L_s\right] = \binom{M}{L_s} q^{L_s}(1-q)^{M-L_s}. \tag{6}$$

D. Optimal Beamforming Weights Design

Our aim is to maximize the received power at the destination in order to maximize the mutual information of the secondary system while limiting the interference to the PU receiver to a tolerable level. Mathematically, the problem formulation for finding the optimal weight vector is described as follows.

$$\begin{aligned} \max_{\mathbf{v}_{opt}, P_r} \quad & P_r|\mathbf{h}^\dagger_{\mathbf{rd}}\mathbf{v}_{opt}|^2 \\ \text{s.t.:} \quad & P_r|\mathbf{h}^\dagger_{\mathbf{rp}}\mathbf{v}_{opt}|^2 \leq Q, \\ & \|\mathbf{v}_{opt}\|^2 = 1, P_r \leq P_v. \end{aligned} \tag{7}$$

To solve the above problem, we first find the optimal beamforming vector $\mathbf{v}_{opt}$, and then the transmit power of the relays $P_r \leq P_v$, is found such that the interference constraint is satisfied, where P_v is the total available power at the relays. We decompose $\mathbf{v}_{opt}$ as a linear combination of two orthonormal vectors, namely, $\mathbf{v}_{opt} = \alpha_v\mathbf{w_{zf}} + \beta_v\mathbf{w_o}$, where α_v and β_v are complex valued weights with $|\alpha_v|^2 + |\beta_v|^2 = 1$ to keep $\|\mathbf{v}_{opt}\|^2 = 1$.

For the zero-interference constraint case, i.e., $Q = 0$, the optimal beamforming vector is the ZFB vector, i.e., $\mathbf{v}_{opt} = \mathbf{w_{zf}}$. According to the ZFB principles, $\mathbf{w_{zf}}$ is chosen to lie in the orthogonal space of $\mathbf{h}^\dagger_{\mathbf{rp}}$ such that $|\mathbf{h}^\dagger_{\mathbf{rp}}\mathbf{w_{zf}}| = 0$ and $|\mathbf{h}^\dagger_{\mathbf{rd}}\mathbf{w_{zf}}|$ is maximized. By applying a standard Lagrangian multiplier method, the weight vector that satisfies the above optimization method is given as

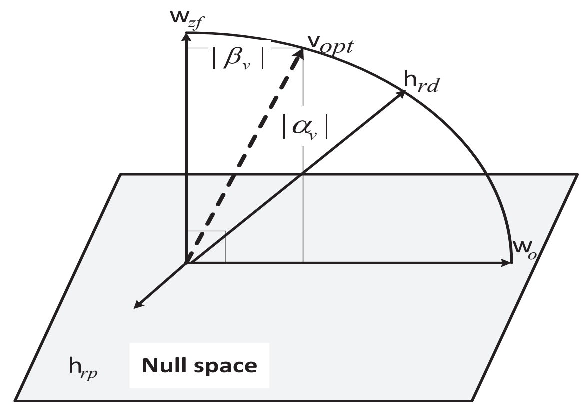

Fig. 2. Geometric explanation of $\mathbf{v}_{opt}$.

$$\mathbf{w_{zf}} = \frac{\mathbf{T}^\perp\mathbf{h_{rd}}}{\|\mathbf{T}^\perp\mathbf{h_{rd}}\|}, \tag{8}$$

where $\mathbf{T}^\perp = \left(\mathbf{I} - \mathbf{h_{rp}}(\mathbf{h}^\dagger_{\mathbf{rp}}\mathbf{h_{rp}})^{-1}\mathbf{h}^\dagger_{\mathbf{rp}}\right)$ is the projection idempotent matrix with rank $(L_s - 1)$.

For the non-zero interference constraint, the secondary relays can increase their transmit power in their own direction, i.e., $\mathbf{h_{rd}}$ while the interference to the PU is constrained to a predefined threshold. Generally, in this case, the beamforming vector is not in the null space of $\mathbf{h_{rp}}$ and since $\mathbf{w}^\dagger_{\mathbf{zf}}\mathbf{w_o} = 0$, we have

$$\mathbf{w_o} = \frac{\mathbf{h_{rd}} - \mathbf{w}^\dagger_{\mathbf{zf}}\mathbf{h_{rd}}\mathbf{w_{zf}}}{\sqrt{1 - |\mathbf{w}^\dagger_{\mathbf{zf}}\mathbf{h_{rd}}|^2}}. \tag{9}$$

By finding $\mathbf{w_{zf}}$ and $\mathbf{w_o}$, the optimal weights are derived as $|\beta_v| \leq \sqrt{\frac{Q}{P_r|\mathbf{h_{rp}}|^2}}$, $\alpha_v = \frac{\mathbf{w}^\dagger_{\mathbf{zf}}\mathbf{h_{rd}}}{|\mathbf{w}^\dagger_{\mathbf{zf}}\mathbf{h_{rd}}|}\sqrt{1-\beta_v^2}$ and $P_r = \frac{Q}{|\mathbf{h_{rp}}|^2}$. To elaborate, a geometric explanation of $\mathbf{v}_{opt}$ is given in Fig. 2 where by rotating $\mathbf{v}_{opt}$ from the ZFB vector $\mathbf{w_{zf}}$ toward the maximum ratio transmission (MRT) beamformer $\mathbf{h_{rd}}$, the secondary relays can maximize the SNR received at the secondary destination at the expense of increasing the interference to the PU while still respecting a predefined threshold Q. In the case of MRT, $\mathbf{v}_{opt} = \mathbf{h_{rd}}$, and therefore the interference constraint becomes irrelevant (non-cognitive case).

Although the optimal scheme yields the maximum SNR at the secondary receiver, it is not commonly used due to its intractability, both in terms of design complexity and performance analysis. As an alternative, ZFB is widely used for its simplicity and low complexity, which is attributed to the fact that designing the ZFB vector involves only a projection of the interference channel vector onto the null space without the extra complexity of computing α_v and β_v. Moreover, as we will demonstrate later, simulation results suggest that there is a little difference in performance between ZFB (given by (8)) and the non-zero interference constraint with α_v and β_v. Motivated by this, for the analysis part, we only consider $\mathbf{w_{zf}}$ because it enables us to obtain closed-form expressions and get insights on the asymptotic performance of the underlying system, which will not be possible otherwise.[3]

III. Performance Analysis of the SDF scheme

In this section, we investigate the SDF relaying protocol employed jointly with ZFB. We consider the SDF scheme where only a set of potential relays who have strong channel conditions to the source and perfectly decode the source's message participate in the second phase. In the first phase, when SS broadcasts a signal x_s to the M relays, the received signal at the ith relay is given as

$$y_r = \sqrt{P} h_{s,r_i} x_s + \sqrt{P_{int}}\ \ g_{m,r_i} x_p + n_r, \tag{10}$$

where n_r denotes the noise at each R_i with variance σ^2 and x_p is the PU's signal. For the second phase, when the potential relays forward the SS's signal after applying ZFB, the received signal at the SD is given as

$$y_d = \sqrt{P_r} \mathbf{h}_{\mathbf{rd}}^{\dagger} \mathbf{w}_{\mathbf{zf}} x_s + \sqrt{P_{int}}\ \ g_{m,d} x_p + n_d, \tag{11}$$

where x_s is the decoded symbol with E $\left[|x_s|^2\right] = \left[|x_p|^2\right] = 1$, and n_d denotes the noise at SD with variance σ^2.

A. End-to-End Received SINR Statistics

We substitute (8) into (11) to get the conditional received SINR as

$$\hat{\gamma}_{eq|\mathcal{C}}^{DF} = \frac{P_r ||\mathbf{T}^{\perp} \mathbf{h}_{\mathbf{r},\mathbf{d}}||^{\mathbf{2}}}{P_{int}|g_{m,d}|^2 + \sigma^2}. \tag{12}$$

To analyze the system, we need to obtain the PDF and CDF of $\hat{\gamma}_{eq|\mathcal{C}}^{DF}$. Let $X = P_r ||\mathbf{T}^{\perp}\mathbf{h}_{\mathbf{r},\mathbf{d}}||^{\mathbf{2}}$ and $Y = P_{int}|g_{m,d}|^2$. Now we have the following *Lemma*.

Lemma 2: Let each entry of $\mathbf{h}_{\mathbf{rd}}$ be i.i.d. $\mathcal{CN} \sim (0, 1)$, then $\left\|\mathbf{T}^{\perp}\mathbf{h}_{\mathbf{rd}}\right\|^2$ is a chi-square random variable with $2(L_s - 1)$ degrees of freedom [23, Theorem 2 Ch.1] with CDF is given as

$$F_{X|\mathcal{C}}(\gamma) = 1 - \frac{1}{(L_s - 2)!}\Gamma\left(L_s - 1, \frac{\gamma}{\gamma_r}\right),\ \gamma \geq 0, \tag{13}$$

where $\gamma_r = \frac{P_r}{\sigma^2}$ and $\Gamma(.,.)$ is the upper incomplete Gamma function defined in [28]. Accordingly, the PDF of $f_{\gamma_{eq|\mathcal{C}}}^{DF}(\gamma)$ is given as

$$f_{X|\mathcal{C}}(\gamma) = \frac{(\gamma)^{L_s-2} e^{-\frac{\gamma}{\gamma_r}}}{(L_s-2)!(\gamma_r)^{L_s-1}},\ \gamma \geq 0,\ L_s \geq 2. \tag{14}$$

Incorporating (14) and the PDF of the exponential random variable Y into the integral of [27, Eq. 6.60], and using [28, 3.326.2], the PDF of $\hat{\gamma}_{eq}^{DF}$ conditional on $\mathcal{C}$ is given as

$$f_{\hat{\gamma}_{eq|\mathcal{C}}^{DF}}(\gamma) = \frac{\zeta \gamma^{\varphi-1}}{\left(\frac{\gamma}{P_r} + \frac{\lambda_{m,d}}{P_{int}}\right)^{\varphi+1}}, \tag{15}$$

where $\zeta = \frac{\lambda_{m,d}}{\Gamma(\varphi) P_{int} (P_r)^{\varphi}}$ and $\varphi = L_s - 1$. Finally, the unconditional PDF of the total received SINR, denoted by γ_{tot}, is written as

$$\begin{aligned} f_{\gamma_{tot}^{DF}}(\gamma) &= \sum_{L_s=0}^{1} \binom{M}{L_s} q^{M-L_s}(1-q)^{L_s}\delta(\gamma) \\ &+ \sum_{L_s=2}^{M} \binom{M}{L_s} q^{M-L_s}(1-q)^{L_s} \frac{\zeta\gamma^{L_s-2}}{\left(\frac{\gamma}{P_r} + \frac{\lambda_{m,d}}{P_{int}}\right)^{L_s}}, \end{aligned} \tag{16}$$

where $\delta(\,.\,)$ is the Dirac function that refers to the received SINR when the relays are inactive.

To compute $F_{\gamma_{tot}^{DF}}(\gamma)$, we integrate (17) which, with the help of [28, 3.194.1], results in

$$\begin{aligned} F_{\gamma_{tot}^{DF}}(\gamma) &= \sum_{L_s=0}^{1} \binom{M}{L_s} q^{M-L_s}(1-q)^{L_s} + \sum_{L_s=2}^{M} \binom{M}{L_s} \\ &\times\ q^{M-L_s}(1-q)^{L_s}\xi\gamma^{\varphi} \\ &\times\ {}_2F_1\left(L_s, \varphi; L_s; -\frac{P_{int}\gamma}{\lambda_{m,d}P_r}\right), \end{aligned} \tag{17}$$

where $\xi = \frac{(P_r)\lambda_{m,d}^{\varphi+2}}{\Gamma(\varphi+1)P_{int}^{\varphi+1}}$ and ${}_2F_1(\,.\,)$ is a Gauss-hypergeometric function defined in [28, Eq. 9.11].

B. Outage Probability Analysis

In this section, we analyze the secondary outage performance. To this end, the mutual information at SD, I_{DF}, can be written as [4]

$$I_{DF} = \frac{1}{2}\log_2\left(1 + \sum_{i\in\mathcal{C}} \gamma_i\right), \tag{18}$$

where γ_i represents the received SNR for each relay-destination link. An outage event occurs when I_{DF} falls below a certain target rate. For a given rate R_{min}, the outage probability, P_{out}, can be rewritten using the total probability theorem as

$$P_{out}^{DF} = \sum_{L_s=0}^{M} \Pr(|\mathcal{C}| = L_s)\Pr(I_{DF} < R_{min}|\,|\mathcal{C}| = L_s). \tag{19}$$

There exist two exclusive outage events for the secondary system with distributed ZFB. Event A: failing to apply ZFB when $L_s < 2$,[4] and Event B: failing to achieve the target rate when $L_s \geq 2$. The probability of event A is

$$\Pr(\text{A}) = \sum_{L_s=0}^{1} \binom{M}{L_s} q^{L_s}(1-q)^{M-L_s}, \tag{20}$$

and the probability of event B is

$$\begin{aligned} \Pr(\text{B}) &= \Pr(I_{DF} < R_{min}|\,|\mathcal{C}| = L_s) \\ &= \Pr\left[\frac{1}{2}\log_2(1+\hat{\gamma}_{eq|\mathcal{C}}^{DF}) < R_{min}\right] = F_{\hat{\gamma}_{eq|\mathcal{C}}^{DF}}(\gamma_{min}), \end{aligned} \tag{21}$$

where $\gamma_{min} = 2^{2R_{min}} - 1$.

Then, from (17), the outage probability is simply given by

$$P_{out}^{DF} = F_{\gamma_{tot}^{DF}}(\gamma_{min}). \tag{22}$$

[3]To be able to apply ZFB, we consider the general assumption that the number of relays must be greater than or equal to the number of primary receivers plus the secondary destination, hence $L_s \geq 2$.

For the case of $P_{int} = 0$, the outage probability for the AWGN scenario is given as

$$P_{out}^{DF} = 1 - \sum_{L_s=2}^{M} \binom{M}{L_s} q^{L_s}(1-q)^{M-L_s} \left(\frac{\Gamma(L_s-1, \frac{\gamma_{min}}{\gamma_r})}{(L_s-2)!} \right). \tag{23}$$

Diversity Gain: To gain some insight about the achievable diversity order, we investigate two cases. The first case is when a fixed power constraint is imposed, i.e., Q is fixed and the second case is when a proportional interference constraint is imposed, i.e., $Q = aP_s$.

In the first case, i.e., when $Q \to \infty$ and $P_s \ll Q$, (18) reduces to

$$P_{out}^{high} \approx \sum_{L_s=0}^{M} \binom{M}{L_s} \left(1 - e^{-\frac{\gamma_{min}\lambda_{s,p}}{\gamma_s}}\right)^{M-L_s} \times \left(e^{-\frac{\gamma_{min}\lambda_{s,p}}{\gamma_s}}\right)^{L_s} \left(\frac{\gamma(L_s-1, \frac{\gamma_{min}}{\gamma_r})}{(L_s-2)!} \right). \tag{24}$$

It is interesting to observe from (24) that the outage probability results in a non-zero constant value. This means that P_{out} saturates when the SU transmit power exceeds the PU threshold. This suggests that the outage probability saturates due to the restriction of Q, leading to a diversity order of zero. Mathematically, the asymptotic diversity order d with respect to Q is given by

$$\begin{aligned} d &= \lim_{Q\to\infty} - \frac{\log\ (P_{out}^{high})}{\log\ (Q)} \\ &= \lim_{Q\to\infty} - \frac{\log(K)}{\log\ (Q)} = 0, \end{aligned} \tag{25}$$

where K is a non-zero constant. Noting that $\lambda_{r,p}, \gamma_s, L_s, \gamma_{min}$ are all constants and using (24), we arrive at (25). Hence, the diversity order is zero in this case.

For the second case, that is, for low to medium values of Q, we assume that Q scales with the maximum power level P_s, i.e., $Q = aP_s$, which effectively neglects the effect of the interference constraint by allowing a large transmit power. The objective here is to examine the achievable diversity for this range of Q. To this end, we first represent (3) in the following form to ease the expansion at high SNRs

$$F_{\gamma_{s,r_i}}(\gamma) = \left(1 - e^{-\frac{Q\lambda_{s,r_i}}{P_s}}\right)\left(1 - e^{-\frac{\sigma^2\gamma\lambda_{s,p}}{P_s}}\right) + e^{-\frac{Q\lambda_{s,r_i}}{P_s}} \left(1 - \frac{Q\lambda_{s,r_i} e^{-\frac{\sigma^2\gamma\lambda_{s,p}}{P_s}}}{\lambda_{s,p}\sigma^2\gamma + Q\lambda_{s,r_i}}\right). \tag{26}$$

For sufficiently high SNR, i.e., as $P_s \to \infty$, using Taylor series expansion, (26) can asymptotically be expressed as

$$F_{\gamma_{s,r_i}}(\gamma) \approx \frac{\sigma^2\gamma\lambda_{s,p}}{P_s} + e^{-\frac{\lambda_{s,r_i}Q}{P_s}} \frac{\sigma^2\gamma\lambda_{s,p}}{Q\lambda_{s,r_i}}. \tag{27}$$

[4]In this case, the system can limit the interference following the same approach used in the first phase. This case was studied in [8].

Substituting $Q = aP_s$ and $\gamma = \gamma_{min}$ into (27), the approximate outage probability expression is given as

$$\begin{aligned} P_{out}^{high} &\approx \sum_{L_s=0}^{M} \binom{M}{L_s} \left(1 - \psi\frac{1}{P_s}\right)^{L_s} \left(\psi\frac{1}{P_s}\right)^{M-L_s} \\ &\quad \times \left(\frac{\gamma(L_s-1, \frac{\gamma_{min}}{\gamma_r})}{(L_s-2)!} \right). \\ &\approx G_a \left(\frac{1}{P_s}\right)^{M-1}, \end{aligned} \tag{28}$$

where $\psi = \sigma^2\lambda_{s,p}\gamma_{min} + e^{-a\lambda_{s,r_i}} \frac{\sigma^2\lambda_{s,p}\gamma_{min}}{a\lambda_{s,r_i}}$ and $G_a = \sum_{L_s=0}^{M} \binom{M}{L_s} \psi^M \left(\frac{\gamma(L_s-1, \frac{\gamma_{min}}{\gamma_r})}{(L_s-2)!} \right)$. Note that (28) suggests that the diversity gain is achieved with order $d = M - 1$ in this case.

C. Bit Error Rate Analysis

We analyze the BER performance due to the errors occurring at SD assuming that all participating relays have accurately decoded and regenerated the message. As such, the BER analysis follows similar lines like those of the outage probability. In particular, the error probability at SD can be written as

$$P_e^{DF} = \sum_{L_s=0}^{M} \Pr(|\mathcal{C}| = L_s)\Pr(P_e||\mathcal{C}| = L_s), \tag{29}$$

where $\Pr(P_e||\mathcal{C}| = L_s)$ is the error probability conditioned on $|\mathcal{C}| = L_s$. The SER could be evaluated using the following identity

$$P_{SER}^{DF} = \frac{a\sqrt{b}}{2\sqrt{\pi}} \int_0^\infty \frac{e^{-bu}}{\sqrt{u}} F_{\gamma_{tot}^{DF}}(u)du, \tag{30}$$

where (a,b) depends on the modulation scheme.

Theorem 1: A closed-form expression for the BER for the SDF-ZFB with the effect of the CCI of the PU is given by

$$\begin{aligned} P_e^{DF} &= \frac{1}{2} \sum_{L_s=0}^{1} \binom{M}{L_s} q^{M-L_s}(1-q)^{L_s} + \epsilon\, \varpi \sum_{L_s=2}^{M} \binom{M}{L_s} \\ &\quad \times q^{M-L_s}(1-q)^{L_s} \Sigma^\nu G_{2,3}^{3,1}\left(-\frac{\nu\, b\, \lambda_{m,d} P_r}{P_{int}} \Big|_{0,\frac{1}{2},-\frac{1}{2}}^{\frac{1}{2}-\varphi,\frac{1}{2}} \right), \end{aligned} \tag{31}$$

where $\Sigma = \left(\frac{\lambda_{m,d}P_r}{P_{int}}\right)$, $\varpi = \frac{a\sqrt{b}}{2\sqrt{\pi}} \frac{\lambda_{m,d}}{P_{int}\Gamma(\varphi)P_r^{\varphi}}$, $\nu = \varphi + \frac{3}{2}$, $\epsilon = \frac{\varphi P_{int}}{\Gamma(L_s)P_r}$ and $(a, b) = (1, 1)$ for BPSK.

Proof: See Appendix B. ∎

In the following, we analyze the BER using BPSK and the SER using M_q-QAM for the AWGN scenario, where M_q is the constellation size.

BER of BPSK: This probability could be evaluated by averaging the error probability P_e over the PDF in (14). Since P_e depends on the modulation scheme, many expressions can be used. In the case of BPSK, $P_e = Q(\sqrt{2\gamma_{eq|\mathcal{C}}^{DF}})$ where $Q(.)$ denotes the $Q-$function defined as $Q(.) = \frac{1}{\sqrt{2\pi}} \int_x^\infty e^{-x^2/2}dx$. After averaging this expression over the

PDF in (14), $\Pr(P_e||\mathcal{C}| = L_s)$ can be calculated as [24, Eq.14-4-15]

$$\Pr(P_e||\mathcal{C}| = L_s) = [\frac{1}{2}(1-\mu)]^{L_s-1} \sum_{k=0}^{L_s-2} \binom{L_s-2+k}{k} \times [\frac{1}{2}(1+\mu)]^k, \quad (32)$$

where $\mu = \sqrt{\frac{\gamma_r}{1+\gamma_r}}$ and $L_s \geq 2$.

Now substituting (32) into (29), P_e^{DF} can be obtained as

$$P_{e_{BPSK}}^{DF} = \frac{1}{2}\sum_{L_s=0}^{1}\binom{M}{L_s} q^{L_s}(1-q)^{M-L_s} + \sum_{L_s=2}^{M}\binom{M}{L_s} \times q^{L_s}(1-q)^{M-L_s}[\frac{1}{2}(1-\mu)]^{L_s-1} \times \sum_{k=0}^{L_s-2}\binom{L_s-2+k}{k}[\frac{1}{2}(1+\mu)]^k, \quad (33)$$

where the first term in the expression appears when the number of selected relays is less than two, hence, we do not have any transmission in the second phase. It is worth noting that the PDF of the received SNR at SD in the non-transmission case (the relay keeps silent) is $\delta(x)$, where $\delta(\cdot)$ is the delta function.

Diversity Gain: Similar to the outage probability case, to analyze the asymptotic behavior of (33), we let $Q \to \infty$ while $P_s \ll Q$. The resulting expression can be expressed as

$$P_e^{high} \approx \sum_{L_s=0}^{M}\binom{M}{L_s}\left(1 - e^{-\frac{\gamma_{min}\lambda_{s,p}}{\gamma_s}}\right)^{M-L_s} \times \left(e^{-\frac{\gamma_{min}\lambda_{s,p}}{\gamma_s}}\right)^{L_s}[\frac{1}{2}(1-\mu)]^{L_s-1} \times \sum_{k=0}^{L_s-2}\binom{L_s-2+k}{k}[\frac{1}{2}(1+\mu)]^k. \quad (34)$$

Mathematically, noting that all $\lambda_{r,p}, \gamma_s, L_s, \gamma_{min}$ are constants, the asymptotic diversity order d with respect to Q is given by

$$d = \lim_{Q\to\infty} -\frac{\log\ (P_e^{high})}{\log\ (Q)} = \lim_{Q\to\infty} -\frac{\log(K)}{\log\ (Q)} = 0, \quad (35)$$

which suggests that the diversity order is zero.

SER of M_q-QAM: For a square M_q-QAM modulation signal ($M_q = 2^k$ with even k), since it can be considered as two independent $\sqrt{k}$-PAM signals, its conditional average SER can be written as

$$P_{e^{DF}_{M_q-QAM}} = \underbrace{\int_0^\infty 4DQ\left(\sqrt{\frac{3}{M_q-1}z}f_{\gamma^{DF}_{eq|\mathcal{C}}}(z)\right)dz}_{I_1} - \underbrace{\int_0^\infty 4D^2Q^2\left(\sqrt{\frac{3}{M_q-1}z}f_{\gamma^{DF}_{eq|\mathcal{C}}}(z)\right)dz}_{I_2} \quad (36)$$

where $D = \left(1 - \frac{1}{\sqrt{M_q}}\right)$. For the first integral I_1, we have

$$I_1 = \frac{2a\sqrt{b}}{\sqrt{\pi}}\int_0^\infty \frac{e^{-bz}}{\sqrt{z}}F_{\gamma^{DF}_{eq|\mathcal{C}}}(z)dz = \frac{2a\sqrt{b}}{\sqrt{\pi}}\int_0^\infty \frac{e^{-bz}}{\sqrt{z}}\frac{\gamma(L_s-1, \frac{z}{\gamma_r})}{(L_s-2)!}dz, \quad (37)$$

where $a = 1 - \frac{1}{\sqrt{M_q}}$ and $b = \frac{3}{2(M_q-1)}$ for M_q-QAM. Using [28, 6.455.2], I_1 results in

$$I_1 = \frac{2a\sqrt{b}}{\sqrt{\pi}}\frac{\Gamma(L_s-\frac{1}{2})(\frac{1}{\gamma_r})^{L_s-1}}{(L_s-1)!(\frac{1}{\gamma_r}+b)^{L_s-\frac{1}{2}}} \times {}_2F_1\left(1, L_s-\frac{1}{2}; L_s; \frac{1}{\gamma_r(\frac{1}{\gamma_r}+b)}\right). \quad (38)$$

For the second integral I_2, we use [32, Eq. 39] as

$$I_2 = \frac{1}{6}a^2\left[3\int_0^\infty e^{-\frac{6}{M_q-1}z}f^{DF}_{\gamma_{eq|\mathcal{C}}}(z)dz + \int_0^\infty e^{-\frac{3}{M_q-1}z}f^{DF}_{\gamma_{eq|\mathcal{C}}}(z)dz\right] = \frac{1}{6}a^2\left[\frac{3}{\gamma_r^{L_s-1}}\left(\frac{6}{M_q-1}+\frac{1}{\gamma_r}\right)^{-L_s+1} + \frac{1}{\gamma_r^{L_s-1}}\left(\frac{3}{M_q-1}+\frac{1}{\gamma_r}\right)^{-L_s+1}\right]. \quad (39)$$

By adding (38) and (39) and following the same steps as in (29), we get a closed-form expression for the SER of M_q-QAM. We note that, in many previous works, I_2 is omitted which may cause a significant error to the SER at low SNRs. In contrast, our closed-form expression gives more accurate results.

IV. Performance Analysis of the AF Scheme

In this section, we consider the AF scheme where a set of relays L_s simply weight and forward the received signals in the second phase. The AF relaying scheme is beneficial in our system model because it is desired to reduce the complexity in CRN. In the proposed setup, in the first phase, the SS broadcasts its signal to all M relays, then the received signal at the ith relay is given in (10). When the potential relays $L_s = M$ participate in the second phase, the received $L_s \times 1$ vector at the relays can be written in a vector form as[5]

$$\mathbf{y_r} = \sqrt{P}\mathbf{h_{sr}}x_s + \mathbf{n_r}, \quad (40)$$

where $\mathbf{h_{sr}}$ is the $L_s \times 1$ source- relays channel vector and $\mathbf{n_r}$ is the relays' noise vector with its elements having variance σ^2. In the second phase, the potential relays amplify and forward the received signals to the destination. To allow concurrent transmission of the secondary relays and PU, we first apply the $L_s \times 1$ ZFB vector denoted by $\mathbf{w_{zf}}$ and then the weighted signals are forwarded to SD. The received signal at SD is given as

$$y_d = \sqrt{P}A_r\mathbf{h}^\dagger_{\mathbf{rd}}\text{Diag}(\mathbf{w_{zf}})\mathbf{h_{sr}}x_s + A_rB_r\mathbf{h}^\dagger_{\mathbf{rd}}\text{Diag}(\mathbf{w_{zf}})\mathbf{n_r} + n_d, \quad (41)$$

[5] In the AF scheme, we do the performance analysis while assuming AWGN because it is mathematically tractable. As for the case with interference, we provide only simulation results because the performance analysis is complex.

where A_r is the normalization constant designed to ensure that the total transmit power at the relays is constrained and it is given by (assuming each R_i knows perfectly h_{s,r_i}) [26]

$$A_r = \sqrt{\frac{P_r}{\mathbf{w_{zf}}^\dagger (P\mathbf{h_{sr}}\mathbf{h}_{\mathbf{sr}}^\dagger + \sigma^2 \mathbf{I})\mathbf{w_{zf}}}}. \quad (42)$$

Then the total received SNR at SD is given as

$$\gamma_{eq}^{AF} = \frac{PA_r^2 |\mathbf{h_{rd}}^\dagger \mathrm{Diag}(\mathbf{w_{zf}})\mathbf{h_{sr}}|^2}{A_r^2 |\mathbf{h_{rd}}^\dagger \mathbf{w_{zf}}|^2 \sigma^2 + \sigma^2}. \quad (43)$$

Now substituting (8) and (42) into (43), and after simple manipulations, the equivalent SNR at SD can be written in the general form of $\gamma_{eq} = \frac{\gamma_1\gamma_2}{\gamma_1+\gamma_2+1}$ as:

$$\gamma_{eq}^{AF} = \frac{\frac{P}{\sigma^2}\left\|\mathbf{h_{sr}}\right\|^2 \gamma_r \left\|\mathbf{T}^\perp \mathbf{h_{rd}}\right\|^2}{\frac{P}{\sigma^2}\left\|\mathbf{h_{sr}}\right\|^2 + \gamma_r \left\|\mathbf{T}^\perp \mathbf{h_{rd}}\right\|^2 + 1}. \quad (44)$$

Considering the peak power constraint on the PU, we express γ_{eq}^{AF} as

$$\gamma_{eq}^{AF} = \begin{cases} \frac{\gamma_s \|\mathbf{h_{sr}}\|^2 \gamma_r \left\|\mathbf{T}^\perp \mathbf{h_{rd}}\right\|^2}{\gamma_s \|\mathbf{h_{sr}}\|^2 + \gamma_r \|\mathbf{T}^\perp \mathbf{h_{rd}}\|^2 + 1}, & P_s < \frac{Q}{|h_{s,p}|^2} \\ \frac{\gamma_q \frac{\|\mathbf{h_{sr}}\|^2}{|h_{s,p}|^2} \gamma_r \left\|\mathbf{T}^\perp \mathbf{h_{rd}}\right\|^2}{\gamma_q \frac{\|\mathbf{h_{sr}}\|^2}{|h_{s,p}|^2} + \gamma_r \|\mathbf{T}^\perp \mathbf{h_{rd}}\|^2 + 1}, & P_s \geq \frac{Q}{|h_{s,p}|^2} \end{cases} \quad (45)$$

where $\gamma_q = \frac{Q}{\sigma^2}$.

A. End-to-End Statistical Analysis of γ_{eq}^{AF}:

We first present the statistics of the new random variables. Then, we derive the CDFs and PDFs of both cases of γ_{eq}^{AF} which will be used in the derivation of the performance metrics. We focus on the analysis of the second case $\left(P_s \geq \frac{Q}{|h_{s,p}|^2}\right)$ as it is more effective and restrictive than the first case $\left(P_s < \frac{Q}{|h_{s,p}|^2}\right)$. It determines the effect of the peak power constraint in the first phase on the performance of the secondary system while the system in the first case becomes a non-cognitive one.

Let $\gamma_1 = \gamma_s \left\|\mathbf{h_{sr}}\right\|^2$, $\gamma_2 = \gamma_r \left\|\mathbf{T}^\perp \mathbf{h_{rd}}\right\|^2$, and $\gamma_3 = \gamma_q \frac{\|\mathbf{h_{sr}}\|^2}{|h_{s,p}|^2}$. We first need to find the CDFs and PDFs for all γ_1, γ_2 and γ_3. The CDF and PDF of γ_2 are given in (13) and (14), respectively, and in the following we derive the PDFs and CDFs of γ_1 and γ_3.

Lemma 3: (PDF and CDF of γ_1): Let each entry of $\mathbf{h_{sr}}$ be i.i.d. $\mathcal{CN} \sim (0,1)$, i.e., $\left\|\mathbf{h_{sr}}\right\|^2$ is a chi-square random variable with $2L_s$ degrees of freedom. Then the PDF and CDF γ_1 are given by

$$f_{\gamma_1}(\gamma) = \frac{(\gamma)^{L_s-1} e^{-\frac{\gamma}{\gamma_s}}}{(L_s-1)!(\gamma_s)^{L_s}}, \ \gamma \geq 0, \quad (46)$$

and

$$F_{\gamma_1}(\gamma) = 1 - \frac{1}{(L_s-1)!}\Gamma\left(L_s, \frac{\gamma}{\gamma_s}\right). \quad (47)$$

Proof: See [25, Chapter 9]. ■

Lemma 4: (PDF and CDF of γ_3): Given that $\left\|\mathbf{h_{sr}}\right\|^2$ is a chi-square random variable with $2L_s$ degrees of freedom (*Lemma 3*), and $|h_{s,p}|^2$ is an exponential random variable, then the PDF and CDF of $\gamma_3 = \gamma_q \frac{\|\mathbf{h_{sr}}\|^2}{|h_{s,p}|^2}$ are given by:

$$f_{\gamma_3}(\gamma) = \frac{\lambda_{s,p} L_s}{(\gamma_q)^{L_s}} \frac{(\gamma)^{L_s-1}}{(\frac{\gamma}{\gamma_q} + \lambda_{s,p})^{L_s+1}}, \quad (48)$$

and

$$F_{\gamma_3}(\gamma) = (\frac{\gamma}{\gamma_q \lambda_{s,p}})^{L_s} \ {}_2F_1(L_s+1, L_s; L_s+1; -\frac{\gamma}{\gamma_q \lambda_{s,p}}), \quad (49)$$

where ${}_2F_1(\, , \, ; \, ; \,)$ is the Gauss hypergeometric function defined in [28].

Proof: See Appendix C. ■

To proceed, we compute the statistics of γ_{eq}^{AF} defined by

$$\gamma_{eq}^{AF} = \frac{\gamma_1 \gamma_2}{\gamma_1 + \gamma_2}, \quad (50)$$

which can be considered as a tractable tight upper bound to the actual equivalent E2E SNR. To this end, γ_{eq}^{AF} in (45) can be rewritten as

$$\gamma_{eq}^{AF} = \begin{cases} \gamma_{eq_1}^{AF}, & P_s < \frac{Q}{|h_{s,p}|^2} \\ \gamma_{eq_2}^{AF}, & P_s \geq \frac{Q}{|h_{s,p}|^2} \end{cases} \quad (51)$$

where $\gamma_{eq_1}^{AF} = \frac{\gamma_s \|\mathbf{h_{sr}}\|^2 \gamma_r \left\|\mathbf{T}^\perp \mathbf{h_{rd}}\right\|^2}{\gamma_s \|\mathbf{h_{sr}}\|^2 + \gamma_r \|\mathbf{T}^\perp \mathbf{h_{rd}}\|^2}$ and $\gamma_{eq_2}^{AF} = \frac{\gamma_q \frac{\|\mathbf{h_{sr}}\|^2}{|h_{s,p}|^2} \gamma_r \left\|\mathbf{T}^\perp \mathbf{h_{rd}}\right\|^2}{\gamma_q \frac{\|\mathbf{h_{sr}}\|^2}{|h_{s,p}|^2} + \gamma_r \|\mathbf{T}^\perp \mathbf{h_{rd}}\|^2}$.

Theorem 2: (CDF of $\gamma_{eq_1}^{AF}$):
The CDF of the tight upper bounded $\gamma_{eq_1}^{AF}$ is given by

$$\begin{aligned} F_{eq_1}^{AF}(\gamma) &= 1 - b\ e^{(-\frac{\gamma}{\gamma_s})} e^{(-\frac{\gamma}{\gamma_r})} \sum_{n=0}^{Ls-2} \sum_{k=0}^{Ls-1} \sum_{v=0}^{k} \binom{L_s-2}{n} \\ &\times \frac{1}{k!}\binom{k}{v} 2(\gamma_r)^{\frac{n-v+1}{2}} (\frac{1}{\gamma_s})^{k+\frac{n-v+1}{2}} (\gamma)^{k+L_s-1} \\ &\times K_{n-v+1}\left(2\sqrt{\frac{\gamma^2}{\gamma_s \gamma_r}}\right), \end{aligned} \quad (52)$$

where $b = \frac{1}{(L_s-2)!\gamma_r^{L_s-1}}$.

Proof: See Appendix D. ■

Theorem 3: (CDF of $\gamma_{eq_2}^{AF}$): The CDF of the tight upper bounded $\gamma_{eq_2}^{AF}$ is given by

$$\begin{aligned} F_{\gamma_{eq_2}}^{AF}(\gamma) &= 1 - d\ e^{(-c\gamma)} \sum_{n=0}^{Ls-1} \sum_{k=0}^{Ls-2} \sum_{v=0}^{k} \frac{1}{k!}\binom{k}{v}\binom{L_s-1}{n} \\ &\times (c)^{k+\frac{n-v}{2}} \Gamma(L_s-n+v)(\gamma)^{L_s-1+k} \\ &\times (\gamma + \lambda_{s,p}\gamma_q)^{\frac{n-v}{2}-L_s} e^{\left(\frac{c\gamma^2}{2(\gamma+\lambda_{s,p}\gamma_q)}\right)} \\ &\times W_{\frac{n-v}{2}-L_s, \frac{-n+v-1}{2}}\left(\frac{c\gamma^2}{(\gamma+\lambda_{s,p}\gamma_q)}\right), \end{aligned} \quad (53)$$

where $d = \frac{\lambda_{s,p}}{\gamma_q}$, $c = 1/\gamma_r$ and $W_{.,.}(.)$ is the Whittaker function defined in [28]. It is worth noting that the Whittaker function is implemented in many mathematical softwares such as Matlab and Mathematica.

Proof: See Appendix E. ■

By differentiating $F_{\gamma_{eq_2}}^{AF}(\gamma)$ with respect to γ, we get the PDF of $\gamma_{eq_2}^{AF}$ which is evaluated numerically and plotted in Fig. 3 for various values of L_s.

B. Moment Generating Function (MGF) of $\gamma_{eq_2}^{AF}$

In order to obtain the average BER for the AF scheme in the second case, the MGF based approach in [25] is used in this paper. Let $\gamma_{eq_2}^{-1} = \gamma_3^{-1} + \gamma_2^{-1} = X_1 + X_2$ where $X_1 = \gamma_3^{-1}$ and $X_2 = \gamma_2^{-1}$. As $\gamma_{eq_2}^{-1}$ is the sum of two independent random

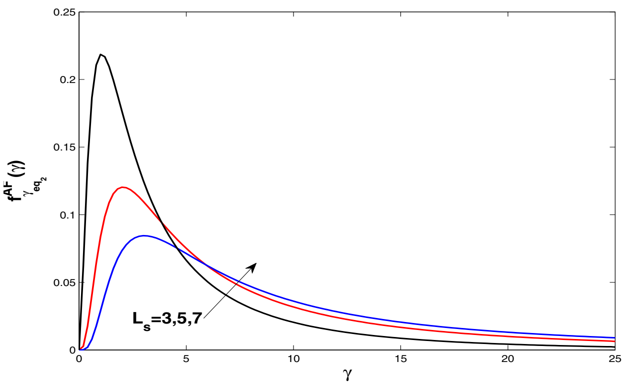

Fig. 3. PDF of the End-to-End received SNR at SD, $f^{AF}_{\gamma_{eq_2}}(\gamma)$ for different values of potential relays in the AF-ZFB scheme for the second case.

variables, the MGF of $\gamma_{eq_2}^{-1}$ results simply from the product of the two MGFs of X_1 and X_2. The MGF of random variable X is defined as

$$\phi_X(s) = E_X\left\{\exp(-sX)\right\} = \int_0^\infty e^{-sz} f_X(z)dz. \tag{54}$$

First, we need to find the PDFs of X_1 and X_2. For the PDF of X_1, we follow the same mathematical approach applied in (79), which after some mathematical manipulations, is obtained as

$$f_{X_1}(z) = \frac{\lambda_{s,p}L_s}{(\gamma_q)^{L_s}}\frac{1}{(\lambda_{s,p}z+\frac{1}{\gamma_q})^{L_s+1}}. \tag{55}$$

The PDF of X_2 is the PDF of the inverse chi-square random variable which leads to the following expression

$$f_{X_2}(z) = \frac{e^{\frac{-1}{\gamma_r z}}}{(\gamma_r)^{L_s-1}(L_s-2)!z^{L_s}}. \tag{56}$$

Substituting (55) into (54), and using [28, 3.382.4], the MGF of X_1 is

$$\phi_{X_1}(s) = \frac{L_s}{(\lambda_{s,p})^{L_s}(\gamma_q)^{L_s}}s^{L_s}e^{\frac{s}{\gamma_q\lambda_{s,p}}}\Gamma(-L_s,\frac{s}{\gamma_q\lambda_{s,p}}). \tag{57}$$

Similarly, substituting (56) into (54), and using [28, 3.471.9], the MGF of X_2 is

$$\phi_{X_2}(s) = \frac{2}{(\gamma_r)^{L_s-1}(L_s-2)!}\left(\frac{s}{\gamma_r}\right)^{\frac{L_s-1}{2}} K_{L_s-1}\left(2\sqrt{\frac{s}{\gamma_r}}\right), \tag{58}$$

where $K_v(.)$ is the modified Bessel function defined in [28]. Now, we can easily compute the MGF of $\gamma_{eq_2}^{-1}$ as the product of $\phi_{X_1}(s)$ and $\phi_{X_2}(s)$ which is given as

$$\begin{aligned}\phi_{\gamma_{eq_2}^{-1}}(s) &= \frac{2L_s}{(\lambda_{s,p})^{L_s}(\gamma_q)^{L_s}(\gamma_r)^{\frac{L_s-1}{2}}(L_s-2)!}s^{\frac{3s-1}{2}}e^{\frac{s}{\gamma_q\lambda_{s,p}}}\\ &\times \Gamma(-L_s,\frac{s}{\gamma_q\lambda_{s,p}})K_{L_s-1}\left(2\sqrt{\frac{s}{\gamma_r}}\right).\end{aligned} \tag{59}$$

We can make use of the following formula to find the MGF of $\gamma_{eq_2}^{AF}$ utilizing the MGF $\gamma_{eq_2}^{-1}$ [29, Eq. 18]

$$\phi_{\gamma_{eq_2}^{AF}}(s) = 1 - 2\sqrt{s}\int_0^\infty J_1(2\beta\sqrt{s})\phi_{\gamma_{eq}^{-1}}(\beta^2)d\beta, \tag{60}$$

where $J_1(.)$ is the Bessel function of the first kind [28]. Although this formula seems to be difficult, we can still use it to study the performance of the BER based on the relationship that exists between the MGF and symbol error rate [25].

C. Outage Probability Analysis

In traditional systems, outage occurs when the received SNR at the destination falls below a pre-determined threshold. However, in spectrum-sharing systems, besides the previous reason, outage occurs when the interference constraint imposed on the secondary transmitters (to limit the inflicted interference on primary users) is not satisfied. Therefore, outage in such systems cannot be avoided. To this end, the mutual information at SD, I_{AF}, can be written as [4]

$$I_{AF} = \frac{1}{2}\log_2(1+\gamma_{eq}^{AF}), \tag{61}$$

where γ_{eq}^{AF} represents the E2E received SNR at SD. An outage event occurs when I_{AF} falls below a certain target rate. For a given rate R_{min}, the outage probability, P_{out}^{AF}, can be rewritten as

$$P_{out}^{AF} = \Pr(I_{AF} < R_{min}) = F_{eq}^{AF}(\gamma_{min}). \tag{62}$$

The corresponding total outage probability for the first case $\left(P_s < \frac{Q}{|h_{s,p}|^2}\right)$ can be computed by substituting (52) into (62), yielding

$$P_{out_1}^{AF} = F_{eq_1}^{AF}(\gamma_{min}), \tag{63}$$

and the corresponding total outage probability for the second case $\left(P_s \geq \frac{Q}{|h_{s,p}|^2}\right)$ can be computed by substituting (53) into (62), and is given as

$$P_{out_2}^{AF} = F_{\gamma_{eq_2}}^{AF}(\gamma_{min}). \tag{64}$$

D. Bit Error Rate Analysis

Exploiting the MGF-based form, the average BER is given by [25]

$$P_e = \frac{1}{\pi}\int_0^{\pi/2}\phi_{\gamma_{eq}}\left(\frac{1}{\sin^2\varphi}\right)d\varphi. \tag{65}$$

Substituting (60) into (65) and after some manipulations, the formula of the BER becomes

$$\begin{aligned}P_e &= \frac{1}{2} - \frac{2}{\pi}\int_0^\infty \phi_{\gamma_{eq}^{-1}}(\beta^2)\int_0^{\pi/2}\left(\sqrt{\frac{1}{\sin^2\varphi}}\right.\\ &\left. J_1\left(2\beta\sqrt{\frac{1}{\sin^2\varphi}}\right)\right)d\varphi d\beta.\end{aligned} \tag{66}$$

The inner integral of (66) can be solved by using change of variables and equation [30, eq. 2.12.4.15] which leads to the value $\frac{\sin(2\beta)}{2\beta}$. So the BER can be evaluated according to the following formula

$$P_e = \frac{1}{2} - \frac{2}{\pi}\int_0^\infty \phi_{\gamma_{eq}^{-1}}(\beta^2)\frac{\sin(2\beta)}{2\beta}d\beta, \tag{67}$$

where $\phi_{\gamma_{eq}^{-1}}$ is the MGF of the inverse SNR given in (59).

Regarding the diversity gain in the AF scheme, in the literature, there were many articles that analyzed the diversity gain especially in traditional and spectrum-sharing systems. Since it is similar to the analysis of the asymptotic behavior of the DF scheme with the same conclusion, we opted for not including it here as it will be a repetition otherwise [18].

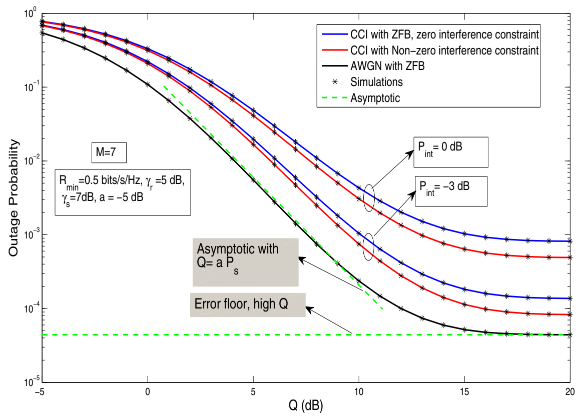

Fig. 4. Outage probability of SDF-ZFB vs. Q(dB) for M=7 and R_{min}= 0.5 bits/s/Hz.

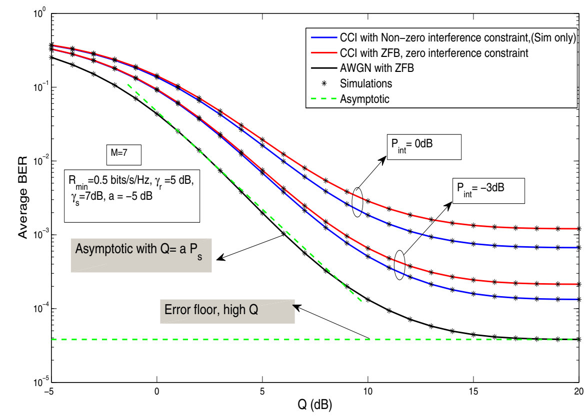

Fig. 6. Average BER of the SDF-ZFB vs. Q for M=7 at R_{min} = 0.5 bit/s/Hz and BPSK scheme.

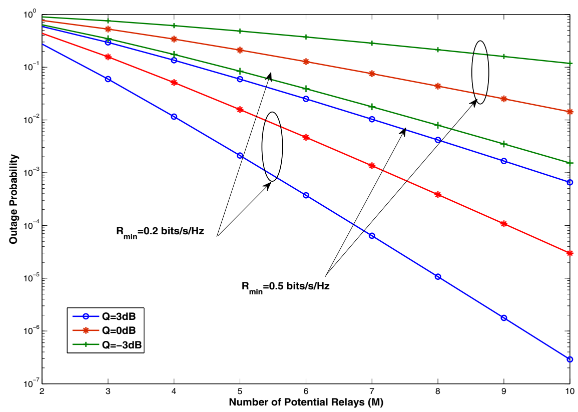

Fig. 5. Outage probability of SDF-ZFB vs. the number of relays for $Q = -3, 0, 3$dB and $R_{min} = 0.2, 0.5$ bits/s/Hz.

V. Numerical Results and Discussions

In this section, we investigate the performance of the derived results numerically and through simulations. For the outage probability analysis, without loss of generality, we assume that $\lambda_{s,p} = \lambda_{s,r_i} = \lambda_{r_i,p} = 1$ and $\lambda_{m,r_i} = \lambda_{m,d} = 1$. We also assume that the maximum transmit powers for the SS and the secondary relays are P_r = 5dB and P_s = 7dB, respectively.

A. SDF scheme

Fig. 4 shows the outage performance of the SDF-ZFB system versus the peak interference level Q at PU for $M = 7$ and R_{min} = 0.5 bits/s/Hz. Clearly, the higher the tolerable interference level, the better the outage performance. The figure also shows that the outage performance saturates at high values of Q which is a result of the limitation on the maximum transmit power of the secondary transmitters. It is obvious that the outage performance with the effect of the CCI from the PU becomes worse than its performance without CCI at the same transmit power and number of relays. The figure also shows the outage performance when a non-zero interference constraint beamforming vector is employed (simulation only). It shows that there is a little difference between the system performance in this case and ZFB due to the loose Q. This appears at high values of Q which is not in the range of operation in cognitive networks.

In Fig. 5, we simulate the outage probability versus the number of potential relays for $Q = -3, 0, 3$ dB and $R_{min} = 0.2, 0.5$ bits/s/Hz. It is clear that by increasing the number of relays that participate in the second phase, the outage performance improves as compared to the non-beamforming SDF case. This is attributed to the fact that applying ZFB acts as an opportunistic relaying in the second phase and it only needs one time slot to transmit as compared to the TDMA schemes that need M time slots.

Fig. 6 illustrates the average BER performance versus Q for M= 7 and R_{min} = 0.5 bits/s/Hz. It is obvious that for low to moderate Q values, the BER improves substantially as the number of potential relays increases and Q becomes less strict. It saturates to a good BER performance for high Q values since the secondary source and the relays transmit at a fixed transmit power as well as maintaining the QoS at the PU. The asymptotic behavior when Q scales with P_s, i.e., $Q = aP_s$ gives a diversity gain with $M - 1$ which emphasizes that the diversity is achieved only in the low transmit power regimes. Moreover, for low value of $P_{int} = -3$ dB, the BER performance with CCI is close to the performance with AWGN only which can happen in practical systems when the PU signal is a Gaussian codeword for instance.

Fig. 7 plots the average SER of the SDF scheme versus Q employing M_q-QAM modulation scheme. We use BPSK, 4-QAM and 16-QAM. Clearly, BPSK gives better performance, however, the 4-QAM and 16-QAM offer better throughput.

Comparison between the outage performances of our system SDF-ZFB and the opportunistic-SDF without the direct path used in [9] and [10] is simulated in Fig. 8. In the figure, we examine the outage probability versus different values of Q with $M = 5, 6$ and maximum transmit power of the secondary transmitters $P_s = 7, 10$ dB at $R_{min} = 0.5$ bits/s/Hz. Our proposed system outperforms the system in [9] and [10] for strict values of Q which is great news as it is more acceptable and practical in cognitive radio systems. For very

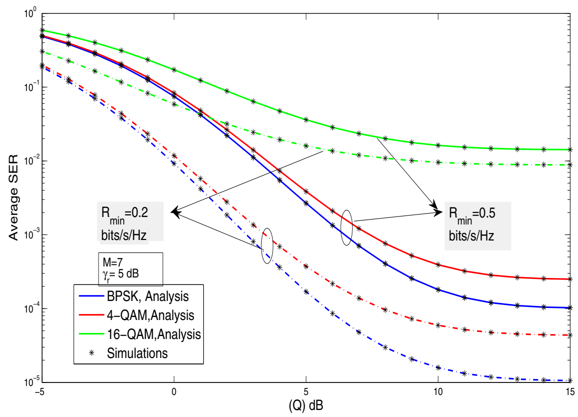

Fig. 7. Average SER of M_q-QAM for the SDF-ZFB vs. Q for M=7 at $R_{min} = 0.2, 0.5$ bit/s/Hz.

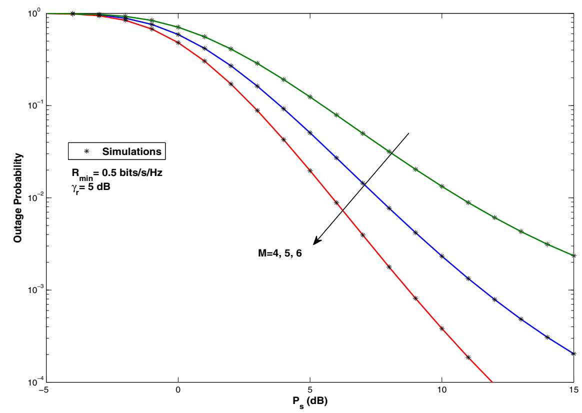

Fig. 9. Outage Probability of AF-ZFB vs. P_s for different number of relays M=4, 5, 6 at R_{min}=0.5 bits/s/Hz in the first case (non-cognitive).

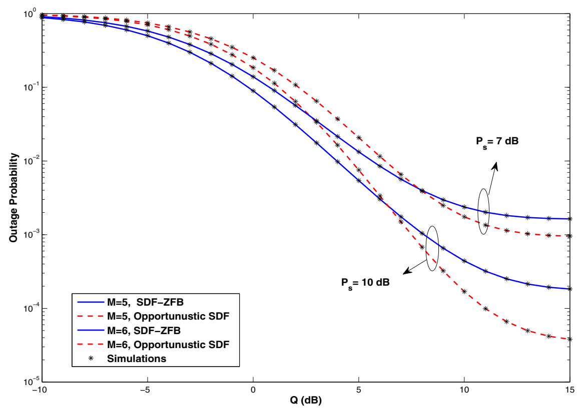

Fig. 8. Comparison between the outage probabilities of SDF-ZFB and the opportunistic SDF presented in [10] for M=5, 6 at R_{min}= 0.5 bits/s/Hz.

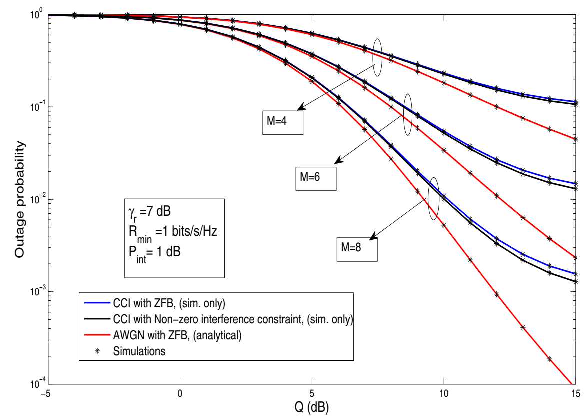

Fig. 10. Outage probability of AF-ZFB vs. Q for M=4, 6, 8 and R_{min}=1 bits/s/Hz in the second case (cognitive).

loose values of Q, the system in [9] and [10] outperforms our proposed system performance. The reason is, at high Q values, their system is described as a non-cognitive system without any interference constraint which is not tolerable in spectrum sharing environments.

B. AF scheme

With the same assumptions as in the SDF scheme, we study the performance of the proposed AF scheme through numerical evaluation and simulations. Fig. 9 shows the outage performance of AF-ZFB for the first case versus the maximum transmit power of the SS for $M = 4, 5, 6$ and $R_{min} = 0.5$ bits/s/Hz at $\gamma_r = 5$ dB. The behavior of the system in this case is the same as the non-cognitive system as it is now free from the interference constraint, and hence, its performance is better than the cognitive ones.

Fig. 10 shows the outage performance of AF-ZFB for the second case versus Q for $M = 4, 6, 8$ and $R_{min} = 0.5, 1$ bits/s/Hz. It can be seen that as the values of Q become less restrict, the outage performance improves substantially. Moreover, by increasing the number of potential relays with ZFB, we observe significant improvements in the outage performance. It is translated to the effect of the combined cooperative diversity and beamforming on enhancing the total received SNR and the mutual information. We also simulate the outage performance considering the PU's CCI in both ZFB and non-zero interference constraint cases. The figure shows that an error floor occurs in the CCI case due to the presence of interference. In the case of AWGN, however, there is no such saturation since there is also no limitation on the maximum transmit power of SS.

Fig. 11 illustrates the average BER performance for the second case versus the interference threshold Q for M= 6, 8, 10 and $\gamma_r = 3, 7$ dB at $R_{min} = 1$ bits/s/Hz. It is obvious that the BER improves substantially as the number of potential relays increases and Q becomes looser. The same interpretation as in Fig. 11 still holds.

Fig. 12 illustrates the average BER for the two schemes versus Q at $R_{min} = 0.5$ bits/s/Hz for $M = 4, 5$. It can be seen that SDF-ZFB outperforms AF-ZFB for low to moderate values of Q and both are similar at high values of Q.

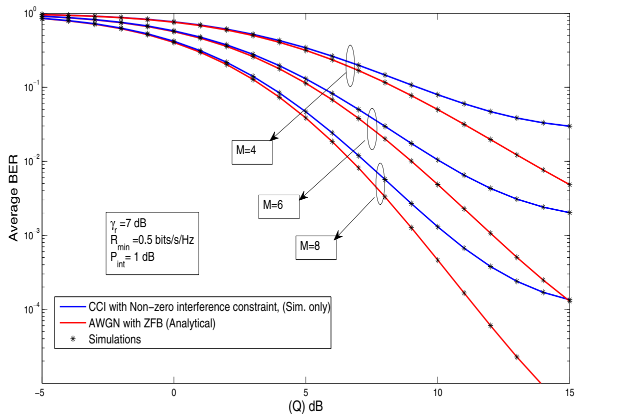

Fig. 11. Average BER of AF-ZFB vs. Q(dB) for M=4, 6, 8 at $R_{min} = 0.5$ bits/s/Hz and $\gamma_r = 7$ dB.

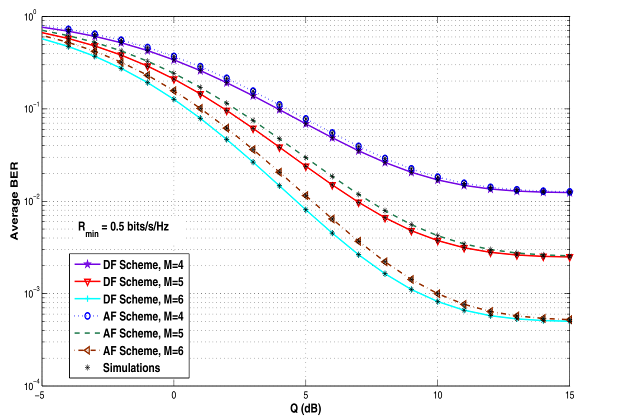

Fig. 12. Comparison between the BER of AF-ZFB and SDF-ZFB for M=4, 5, 6 at R_{min}=0.5 bits/s/Hz.

VI. Conclusion

We considered cooperative relaying and distributed beamforming for spectrum sharing systems with the objective of improving the performance of the secondary system while respecting the interference constraint imposed by the PU. We considered both DF and AF relaying. The optimal beamforming weights were derived to maximize the received SNR at the secondary destination while the interference to the PU is kept to a predefined threshold. Given the high complexity of using optimal beamforming in the analysis, we adopted ZFB instead. With this, we analyzed the performance of the secondary system by deriving the outage probability and BER. We verified our analytical results through simulations which showed the benefits of our proposed system in improving the secondary system performance by compensating the performance loss due to the PU's CCI. The results showed that distributed ZFB improves the outage probability and BER performance by increasing number of participating relays compared to non-beamforming selection relaying schemes. The results also demonstrated the deteriorating impact of the PU's strict interference threshold and CCI. The results also showed that our proposed SDF-ZFB system outperforms the opportunistic SDF system performance for strict values of the interference constraint.

VII. Appendices

A. Proof of Lemma 1

Let $X = |h_{s,r_i}|^2, Y = |f_{s,p}|^2, Z = P_{int}|g_{m,r_i}|^2 + \sigma^2$, then the CDF of γ_{s,r_i} conditioned on Z is given as

$$F_{\gamma_{s,r_i}|Z}(\gamma) = \underbrace{\Pr\left(\frac{QX}{Y} < Z\gamma, Y \geq \frac{Q}{P_s}\right)}_{I_1(Z)} + \underbrace{\Pr\left(P_s X < Z\gamma, Y < \frac{Q}{P_s}\right)}_{I_2(Z)};$$

$$\begin{aligned} I_1(Z) &= \int_{\vartheta}^{\infty} f_Y(y)\int_0^{\frac{Z\gamma}{Q}y} f_X(x)dxdy \\ &= \int_{\vartheta}^{\infty} f_Y(y)F_X(\frac{Z\gamma}{Q}y)dy, \end{aligned} \tag{68}$$

where $\vartheta = \frac{Q}{P_s}$.
Substituting for the PDF of Y and CDF of X, we derive $I_1(Z)$ as

$$I_1(Z) = 1 - F_Y(\vartheta) - \frac{\lambda_y e^{-(\frac{\lambda_x Z\gamma}{Q}+\lambda_y)\vartheta}}{(\frac{\lambda_x Z\gamma}{Q}+\lambda_y)}, \tag{69}$$

where $\lambda_x = \lambda_{s,r_i}$ and $\lambda_y = \lambda_{s,p}$. Next, due to the statistical independence between X and Y, the second integral $I_2(Z)$ is evaluated as

$$I_2(Z) = F_Y(\vartheta)F_X(\frac{\gamma}{P_s}Z). \tag{70}$$

The unconditional CDF of γ_{s,r_i} is derived by averaging (68) and (69) over the PDF of Z as follows

$$F_{\gamma_{s,r_i}}(\gamma) = \mathrm{E}_Z\left\{F_{\gamma_{s,r_i}|Z}(\gamma)\right\} = I_3 + I_4,$$

where $I_3 = \mathrm{E}_Z\{I_1(Z)\}$ and $I_4 = \mathrm{E}_Z\{I_2(Z)\}$. To proceed, we need the PDF of Z which is given by

$$f_Z(z) = \frac{\lambda_z e^{\frac{\lambda_z\sigma^2}{P_{int}}}}{P_{int}} e^{-\frac{\lambda_z z}{P_{int}}} u(z-\sigma^2), \tag{71}$$

where $\lambda_z = \lambda_{m,r_i}$ and $u(.)$ is the unit-step function. Incorporating (71) into (68), I_3 is derived as

$$\begin{aligned} I_3 &= 1 - F_Y(\vartheta) - \frac{\lambda_y\lambda_z e^{\frac{\lambda_z\sigma^2}{P_{int}}} e^{-\lambda_y\vartheta}}{P_{int}} \\ &\quad \times \underbrace{\int_{\sigma^2}^{\infty}\left(\frac{\lambda_x\gamma z}{Q}+\lambda_y\right)^{-1} e^{-(\frac{\lambda_x\gamma}{Q}+\frac{\lambda_z}{P_{int}})z}dz}_{I_{31}}. \end{aligned} \tag{72}$$

Utilizing [28, Eq. 3.352.2], I_{31} can be computed as follows.

$$\begin{aligned} I_{31} &= \frac{e^{-\lambda_{s,p}\vartheta+\frac{\lambda_{m,r_i}\sigma^2}{P_{int}}}}{\gamma}\left(-e^{\frac{Q\lambda_{s,p}}{\lambda_{s,r_i}\gamma}\left(\frac{\lambda_{m,r_i}}{P_{int}}+\frac{\lambda_{s,r_i}\gamma}{Q}\right)}\right. \\ &\quad \times \left. Ei\left[-\left(\frac{Q\lambda_{s,p}}{\gamma\lambda_{s,r_i}}+\sigma^2\right)\left(\frac{\lambda_{m,r_i}}{P_{int}}+\frac{\lambda_{s,r_i}\gamma}{Q}\right)\right]\right), \end{aligned} \tag{73}$$

where $\frac{Q\lambda_{s,p}\lambda_{m,r_i}}{\lambda_{s,r_i}P_{int}}$. Similarly, to evaluate I_4, we average over $I_2(Z)$ with respect to Z which results in

$$I_4 = F_Y(\vartheta)(\frac{\lambda_{m,r_i}e^{\frac{\lambda_{m,r_i}\sigma^2}{P_{int}}}}{P_{int}})\left(\frac{e^{-\frac{\lambda_{m,r_i}\sigma^2}{P_{int}}}P_{int}}{\lambda_{m,r_i}} - \frac{e^{-\sigma^2\left(\frac{\lambda_{m,r_i}}{P_{int}}+\frac{\lambda_{s,p}\gamma}{P_s}\right)}P_sP_{int}}{P_{int}\lambda_{s,p}\gamma+P_s\lambda_{m,r_i}}\right). \quad (74)$$

Substituting (73) into (72) and adding with (74) results in (2), which concludes the proof.

B. Proof of Theorem 1

First, we represent the Gauss-hypergeometric function in (17) and also the exponential function in (30) in terms of Meijer's G-functions using [31, Eq. 10, 11], which are given, respectively, as

$$2F_1\left(\varphi+1,\varphi;\varphi+1;-\frac{P_{int}u}{\lambda_{m,d}P_r}\right) = \frac{\varphi\, P_{int}\, u}{\Gamma(L_s)P_r} \times G_{2,2}^{1,2}\left(-\frac{P_{int}\,u}{\lambda_{m,d}P_r}\Big|_{-1,-(\varphi+1)}^{-L_s,-\varphi}\right);$$

$$e^{-bu} = G_{0,1}^{1,0}\left(bu|_0^-\right). \quad (75)$$

Thus, integrating the second term of (17) yields

$$J_1 = \varpi\,\epsilon\int_0^\infty\left(u^{\varphi+\frac{1}{2}}G_{2,2}^{1,2}\left(-\frac{P_{int}u}{\lambda_{m,d}P_r}\Big|_{-1,-(\varphi+1)}^{-L_s,-\varphi}\right) \times G_{0,1}^{1,0}\left(bu|_0^-\right)\right)du, \quad (76)$$

where $\varphi = L_s-1$, $\varpi = \frac{a\sqrt{b}}{2\sqrt{\pi}}\frac{\lambda_{m,d}}{P_{int}\Gamma(\varphi)P_r^{\varphi}}$, $\epsilon = \frac{\varphi P_{int}}{\Gamma(L_s)P_r}$.
By exploiting the integral of the product of a power term and two Meijer's G-function in [31, Eq. 21], (76) results in

$$J_1 = \varpi\,\epsilon\left(\frac{\lambda_{m,d}P_r}{P_{int}}\right)^{\nu}G_{2,3}^{3,1}\left(-\frac{\nu\, b\,\lambda_{m,d}P_r}{P_{int}}\Big|_{0,1-\frac{1}{2},-\frac{1}{2}}^{\frac{1}{2}-\varphi,\frac{1}{2}}\right), \quad (77)$$

where $\nu = \varphi+\frac{3}{2}$. Therefore, adding (77) with the first term of (33), a closed-form expression for the unconditional BER at SD is given as in (31). Thus the proof is completed.

C. Proof of Lemma 4

Let $\gamma_1 = (\frac{\gamma_q\|\mathbf{h_{sr}}\|^2}{|h_{s,p}|^2}) = \frac{X}{Y}$. As we mentioned above, $\|\mathbf{h_{sr}}\|^2$ is a chi-square random variable with $2L_s$ degrees of freedom, and $|h_{s,p}|^2$ is an exponential random variable. We use the integral formula from [27, Eq. 6.60] to find the PDF of $f_{\gamma_1}(\gamma)$ as follows

$$f_{\gamma_1}(\gamma) = \int_{y=0}^\infty y f_{\|\mathbf{h_{sr}}\|^2}(y\gamma)f_{|h_{s,p}|^2}(y)dy \quad (78)$$
$$= \frac{\lambda_{s,p}(\gamma)^{L_s-1}}{(\gamma_q)^{L_s}(L_s-1)!}\int_{y=0}^\infty y^{L_s}e^{(-y\gamma/\gamma_q)}e^{-\lambda_{s,p}y}dy.$$

The last integral can be determined using [28, Eq. 3.326.1], resulting in (48).
To find the CDF, we integrate the PDF as follows

$$F_{\gamma_1}(\gamma) = \int_0^\gamma f_{\frac{\|\mathbf{h_{sr}}\|^2}{|h_{s,p}|^2}}(x)dx = \frac{\lambda_{s,p}L_s}{(\gamma_q)^{L_s}}\int_0^\gamma\frac{(x)^{L_s-1}}{(\frac{x}{\gamma_q}+\lambda_{s,p})^{L_s+1}}dx. \quad (79)$$

We use [28, Eq. 3.194.1] to solve the above integral which gives (49).

D. Proof of Theorem 2

In the following, we derive the exact form for the CDF of the equivalent SNR in the form $\gamma_{eq} = \frac{\gamma_1\gamma_2}{\gamma_1+\gamma_2}$. By using the definition of CDF $F_{\gamma_{eq_1}}^{AF}(\gamma) = F\left(\frac{\gamma_1\gamma_2}{\gamma_1+\gamma_2}\le\gamma\right)$, and invoking (13), (14), (46) and (47), $F_{\gamma_{eq_1}}^{AF}(\gamma)$ can be expressed as

$$\begin{aligned}F_{\gamma_{eq_1}}^{AF}(\gamma) &= \int_0^\infty \Pr\left[\frac{\gamma_1\gamma_2}{\gamma_1+\gamma_2}\le\gamma|\gamma_2\right]f_{\gamma_2}(\gamma_2)d\gamma_2\\ &= \int_0^\gamma \Pr\left[\gamma_1\ge\frac{\gamma\gamma_2}{\gamma_2-\gamma}|\gamma_2\right]f_{\gamma_2}(\gamma_2)d\gamma_2\\ &+ \int_\gamma^\infty \Pr\left[\gamma_1\le\frac{\gamma\gamma_2}{\gamma_2-\gamma}|\gamma_2\right]f_{\gamma_2}(\gamma_2)d\gamma_2\\ &= I_1(\gamma)+I_2(\gamma),\end{aligned} \quad (80)$$

where

$$I_1(\gamma) = \int_0^\gamma f_{\gamma_2}(\gamma_2)d\gamma_2 = F_{\gamma_2}(\gamma), \quad (81)$$

which is presented in (13), and

$$I_2(\gamma) = \int_\gamma^\infty F_{\gamma_1}\left(\frac{\gamma\gamma_2}{\gamma_2-\gamma}\right)f_{\gamma_2}(\gamma_2)d\gamma_2. \quad (82)$$

Then, substituting (47) and (14) into (82), $I_2(\gamma)$ becomes

$$\begin{aligned}I_2(\gamma) &= \int_\gamma^\infty\left(1-\frac{\Gamma(L_s,\frac{\gamma}{\gamma_2-\gamma}\frac{\gamma_2}{\gamma_s})}{(L_s-1)!}\right)f_{\gamma_2}(\gamma_2)d\gamma_2\\ &= \int_\gamma^\infty f_{\gamma_2}(\gamma_2)d\gamma_2 - \int_\gamma^\infty\frac{\Gamma\left(L_s,\frac{\gamma}{\gamma_2-\gamma}\frac{\gamma_2}{\gamma_s}\right)}{(L_s-1)!}\times f_{\gamma_2}(\gamma_2)d\gamma_2\\ &= 1-\int_0^\gamma f_{\gamma_2}(\gamma_2)d\gamma_2 - \int_\gamma^\infty\frac{\Gamma\left(L_s,\frac{\gamma}{\gamma_2-\gamma}\frac{\gamma_2}{\gamma_s}\right)f_{\gamma_2}(\gamma_2)}{(L_s-1)!}d\gamma_2.\end{aligned} \quad (83)$$

Then substituting (81) and (83) into (80) yields

$$F_{\gamma_{eq_1}}^{AF}(\gamma) = 1-\underbrace{\int_\gamma^\infty\frac{\Gamma\left(L_s,\frac{\gamma}{\gamma_2-\gamma}\frac{\gamma_2}{\gamma_s}\right)}{(L_s-1)!}f_{\gamma_2}(\gamma_2)d\gamma_2}_{I_3}. \quad (84)$$

By using the variable change $u = \gamma_2 - \gamma$, the integral I_3 can be written as

$$I_3 = a\int_0^\infty \Gamma\left(L_s, c_o\gamma + \frac{c_o\gamma^2}{u}\right)\frac{(u+\gamma)^{L_s-2}e^{-\frac{u+\gamma}{\gamma_r}}}{(L_s-2)!(\gamma_r)^{L_s-1}}du, \tag{85}$$

where $a = \frac{1}{(L_s-2)!(L_s-1)!\gamma_r^{L_s-1}}$ and $c_o = 1/\gamma_s$.
By using [28, Eq. 8.352.2] and [28, Eq. 1.111], the incomplete gamma function of the integral in (85) can be expressed as

$$\begin{aligned}\Gamma(L_s-1, c_o\gamma + \frac{c_o\gamma^2}{u}) &= (Ls-2)!e^{\left(-c_o\gamma - \frac{c_o\gamma^2}{u}\right)} \\ &\times \sum_{k=0}^{Ls-2}\sum_{v=0}^{k}\frac{1}{k!}\binom{k}{v}(c_o\gamma)^{k-v} \\ &\times (c_o\gamma^2)^v\frac{1}{(u)^v}. \end{aligned}\tag{86}$$

By using [28, Eq. 1.111] again for the term $(u+\gamma)^{L_s-2}$, I_3 can be expressed as

$$\begin{aligned}I_3 &= a\ (Ls-2)!e^{(-\frac{\gamma}{\gamma_s})}\sum_{n=0}^{Ls-2}\sum_{k=0}^{Ls-1}\sum_{v=0}^{k}\frac{1}{k!}\binom{k}{v}\binom{L_s-2}{n} \\ &\times (c_o)^k\int_0^\infty e^{\left(-\frac{\gamma^2}{\gamma_s u}\right)}(u)^{n-v}e^{-\frac{u}{\gamma_r}}du \\ &\times (\gamma)^{L_s-2-n}(\gamma)^{k+v}e^{-\frac{\gamma}{\gamma_r}}. \end{aligned}\tag{87}$$

The inner integral of I_3 can be solved by exploiting [28, Eq. 3.471.9], resulting in

$$\begin{aligned}I_3 &= a\ (Ls-2)!e^{(-\frac{\gamma}{\gamma_s})}\sum_{n=0}^{Ls-2}\sum_{k=0}^{Ls-1}\sum_{v=0}^{k}\frac{1}{k!}\binom{k}{v}\binom{L_s-2}{n} \\ &\times (\gamma)^{L_s-2-n}(\gamma)^{k+v}e^{-\frac{\gamma}{\gamma_r}}2(\gamma_r)^{\frac{n-v+1}{2}}(\frac{1}{\gamma_s})^{k+\frac{n-v+1}{2}} \\ &\times (\gamma)^{n-v+1}K_{n-v+1}\left(2\sqrt{\frac{\gamma^2}{\gamma_s\gamma_r}}\right). \end{aligned}\tag{88}$$

With the help of (84) and (88) and after some mathematical manipulations, we get the exact CDF expression of the equivalent SNR $F^{AF}_{\gamma_{eq_1}}(\gamma)$ as in (52).

E. Proof of Theorem 3

Following the same approach as in the *Proof of Theorem 2* and after some mathematical manipulations, we obtain the exact CDF expression of the equivalent SNR $F^{AF}_{\gamma_{eq_2}}(\gamma)$ as given in (53).

References

[1] S. Haykin, "Cognitive radio: brain-empowered wireless communications," *IEEE J. Sel. Areas Commun.,* vol. 23, no. 9, pp. 201–220, 2005.

[2] A. Goldsmith, S. A. Jafar, I. Maric, and S. Srinivasa, "Breaking spectrum gridlock with cognitive radios: an information theoretic perspective," *Proc. IEEE,* vol. 97, no. 5, pp. 894–914, May 2009.

[3] T. M. Duman and A. Ghrayeb, *Coding for MIMO Communication Systems.* Wiley & Sons, 2008.

[4] J. N. Laneman, D. N. C Tse, and G. W. Wornell, "Cooperative diversity in wireless networks: efficient protocols and outage behavior," *IEEE Trans. Inf. Theory,* vol. 50, no. 12, pp. 3062–3080, Dec. 2004.

[5] X. Zeng, A. Ghrayeb, and M. Hasna, "Joint optimal threshold-based relaying and ML detection in network-coded two-way relay," *IEEE Trans. Commun.,* vol. 60, no. 9, pp.2657–2667, Sept. 2012.

[6] X. Zhang, M. Hasna, and A. Ghrayeb, "Performance analysis of relay assignment schemes for cooperative networks with multiple source-destination pairs," *IEEE Trans. Wireless Commun.,* vol. 11, no. 1, pp. 166–177, Jan. 2012.

[7] S. Nguyen, A. Ghrayeb, G. Al-Habian, and M. Hasna, "Mitigating error propagation in two-way relay channels employing network coding," *IEEE Trans. Wireless Commun.,* vol. 9, no. 11, pp. 3380–3390, Nov. 2010.

[8] V. Asghari and S. Aissa, "End-to-End performance of cooperative relaying in spectrum-sharing systems with quality of service requirements," *IEEE Trans. Veh. Technol.,* vol. 60, no. 6, pp. 2656–2668, July 2011.

[9] Y. Guo, G. Kang, Q. Sun, M. Zhang, and P. Zhang, "Outage performance of cognitive-radio relay system based on the spectrum-sharing environment," in *Proc. 2010 IEEE GLOBECOM,* pp. 1–5.

[10] Z. Yan, X. Zhang, and W. Wang, "Exact outage performance of cognitive relay networks with maximum transmit power limits," *IEEE Commun. Lett.,* vol. 15, no. 12, pp. 1317–1319, Dec. 2011.

[11] S. Sanguk, J. Lee, and D. Hong, "Capacity of reactive DF scheme in cognitive relay networks," *IEEE Trans. Wireless Commun.,* vol. 10, no. 10, pp. 3133–3138, Oct. 2011.

[12] K. Zarifi, A. Ghrayeb, and S. Affes, "Jointly optimal source power control and relay matrix design in multipoint-to-multipoint cooperative communication networks," *IEEE Trans. Signal Process.,* vol. 59, no. 9, pp. 4313–4330, Sept. 2011.

[13] J. Habibi, A. Ghrayeb, and A. G. Aghdam, "Energy-efficient cooperative routing in wireless sensor networks: a mixed-integer optimization framework and explicit solution," *IEEE Trans. Commun.*, vol. 61, no. 8, pp. 3424–3437, Aug. 2013.

[14] K. Hamdi, K. Zarifi, K. Ben Letaief, and A. Ghrayeb, "Beamforming in relay-assisted cognitive radio systems: a convex optimization approach," in *Proc. 2011 IEEE ICC,* pp.1–5, June 2011.

[15] K. Zarifi, S. Affes, and A. Ghrayeb, "Joint source power control and relay beamforming in amplify-and-forward cognitive networks with multiple source-destination pairs," in *Proc. 2011 IEEE ICC,* pp. 5–9.

[16] A. Afana, V. Asghari, A. Ghrayeb, and S. Affes, "Cooperative relaying in spectrum-sharing systems with beamforming and interference constraints," in *Proc. 2012 IEEE SPAWC.*

[17] A. Afana, V. Asghari, A. Ghrayeb, and S. Affes, "Enhancing the performance of spectrum-sharing systems via collaborative distributed beamforming and AF relaying," in *Proc. 2012 IEEE GLOBECOM.*

[18] R. Manna, R. H. Y Louie, Y. Li, and B. Vucetic, "Cooperative spectrum sharing in cognitive radio networks with multiple antennas," *IEEE Trans. Signal Process.,* vol. 59, no. 11, pp. 5509–5522, Nov. 2011.

[19] J. M. Peha, "Approaches to spectrum sharing," *IEEE Commun. Mag.,* vol. 8, no. 1, pp. 10–11, Feb. 2005.

[20] L. Zhang, Y.-C. Liang, and Y. Xin, "Joint beamforming and power allocation for multiple access channels in cognitive radio networks," *IEEE J. Sel. Areas Commun.,* vol. 26, no. 1, pp. 38–51, Jan. 2008.

[21] L. Tong, B. M. Sadler, and M. Dong, "Pilot-assisted wireless transmissions: general model, design criteria, and signal processing," *IEEE Signal Process. Mag.,* vol. 21, no. 6, pp. 12–25, Nov. 2004.

[22] V. Havary-Nassab, S. Shahbazpanahi, and A. Grami, "Optimal distributed beamforming for two-way relay networks," *IEEE Trans. Signal Process.,* vol. 58, no. 3, pp. 1238–1250, Mar. 2010.

[23] R. J. Pavur, "Quadratic forms involving the complex Gaussian," M.Sc. dissertation, Math. Dept., Texas Tech. Univ., Lubbock, TX, Aug. 1980.

[24] J. Proakis, *Digital Communications*, 4th ed. McGraw-Hill, 2000.

[25] M. K. Simon and M.-S. Alouini, *Digital Communications over Fading Channels*, 2nd ed. Wiley, 2005.

[26] R. H. Y Louie, Y. Li, and B. Vucetic, "Zero forcing in general two-hop relay networks," *IEEE Trans. Veh. Technol.,* vol. 59, no. 1, pp. 191–201, Jan. 2010.

[27] A. Papoulis and S. U. Pillai, *Probability, Random Variables, and Stochastic Processes*, 4th ed. McGraw-Hill, 2002.

[28] I. S. Gradshteyn and I. M. Ryzhik, *Table of Integrals, Series and Products*, 7th ed. Elsevier, 2007.

[29] M. Di Renzo, F. Graziosi, and F. Santucci, "A unified framework for performance analysis of CSI-assisted cooperative communications over fading channels," *IEEE Trans. Commun.,* vol. 57, no. 9, pp. 2251–2257, Sep. 2009.

[30] A. P. Prudnikov, Y. A. Brychkov, and O. I. Marichev, *Integrals and Series, Volume 2: Special Functions,* 2nd printing with corrections. Gordon and Breach Science Publishers, 1988.

[31] V. Adamchik and O. Marichev, "The algorithm for calculating integrals of hypergeometric type functions and its realization in reduce systems," in *Proc. 1990 Intern. Conf. Symbolic Algebraic Computation.*

[32] M. Li, M. Lin, Q. Yu, W.-P. Zhu, and L. Dong, "Optimal beamformer design for dual-hop MIMO AF relay networks over Rayleigh fading

channels," *IEEE J. Sel. Areas Commun.,* vol. 30, no. 8, pp. 1402–1414, Sept. 2012.

Ali Afana received the bachelor degree (B.Sc.) in electrical engineering, major Communications and Control, from Islamic University of Gaza-Palestine in 2006 and the M.Sc. degree in communications engineering from Birmingham University, Birmingham, UK in 2009 (with Distinction). He is currently working toward his Ph.D. degree in electrical engineering at Concordia University, Montreal, Quebec, Canada. His research interests span different topics in wireless communications, including signal processing for wireless communications, performance analysis of cooperative relaying in cognitive radio networks, and physical-layer security for massive multi-input multi-output (MIMO) systems.

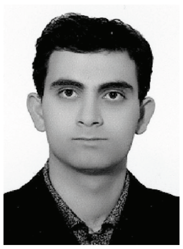

Vahid Reza Asghari (S'07-M'12) obtained his Ph.D. degree in Telecommunications from INRS-EMT, University of Quebec, Montreal, Canada in 2012 and his B.Sc. degree in electrical engineering from Azad University and the M.Sc. degree in telecommunication systems from K.N.Toosi University of Technology in 2002 and 2005, respectively. From 2005 to 2007, he was a Researcher with the department of electrical engineering, K.N.Toosi University of Technology. From 2011 to 2013, he was as a postdoctoral research fellow at INRS-EMT, Montreal, Canada, where he worked on an admission control algorithm for heterogeneous networks. He is currently working as a postdoctoral research fellow at the department of electrical engineering, McGill University, Montreal, Canada. His research interests include resource scheduling and management, cooperative communications with a focus on heterogeneous systems. He is also interested in behavior modeling, analysis and management of smart applications using ICT technology with a focus on cloud computing networks. He is a recipient of Postdoctoral Research Fellowship Award from the Quebec Government Fonds Qubcois de la Recherche sur la Nature et les Technologies (FQRNT), 2012-2014. He is also co-recipient of Best Paper Award from IEEE WCNC 2010.

Ali Ghrayeb received the Ph.D. degree in electrical engineering from the University of Arizona, Tucson, USA in 2000. He is currently a Professor with the Department of Electrical and Computer Engineering, Texas A&M University at Qatar (on leave from Concordia University, Montreal, Canada.)

He is a co-recipient of the IEEE Globecom 2010 Best Paper Award. He is the coauthor of the book Coding for MIMO Communication Systems (Wiley, 2008). His research interests include wireless and mobile communications, error correcting coding, MIMO systems, wireless cooperative networks, and cognitive radio systems.

Dr. Ghrayeb has instructed/co-instructed technical tutorials at several major IEEE conferences. He served as the TPC co-chair of the Communications Theory Symposium of IEEE Globecom 2011. He is serving as the TPC co-chair of the 2016 IEEE WCNC conference. He serves as an Editor of the IEEE TRANSACTIONS ON WIRELESS COMMUNICATIONS, and the IEEE TRANSACTIONS ON COMMUNICATIONS. He served as an Associate Editor of IEEE TRANSACTIONS ON SIGNAL PROCESSING, IEEE TRANSACTIONS ON VEHICULAR TECHNOLOGY, the *Elsevier Physical Communications*, and the *Wiley Wireless Communications and Mobile Computing Journal*.

Sofiène Affes (S'94-M'95-SM'04) received the Diplome d'Ingenieur in telecommunications in 1992, and the Ph.D. degree with honors in signal processing in 1995, both from the Ecole Nationale Suprieure des Telecommunications (ENST), Paris, France.

He has been since with INRS-EMT, University of Quebec, Montreal, Canada, as a Research Associate from 1995 till 1997, as an Assistant Professor till 2000, then as an Associate Professor till 2009. Currently he is a Full Professor in the Wireless Communications Group. His research interests are in wireless communications, statistical signal and array processing and adaptive space-time processing. From 1998 to 2002 he has been leading the radio design and signal processing activities of the Bell/Nortel/NSERC Industrial Research Chair in Personal Communications at INRS-EMT, Montreal, Canada. Since 2004, he has been actively involved in major projects in wireless of PROMPT (Partnerships for Research on Microelectronics, Photonics and Telecommunications).

Professor Affes was the co-recipient of the 2002 Prize for Research Excellence of INRS. From 2003 till 2013, he held a Canada Research Chair in Wireless Communications. From 2008 to 2011, he held a Discovery Accelerator Supplement (DAS) Award from NSERC (Natural Sciences & Engineering Research Council of Canada). Very recently, he has been awarded a second DAS from NSERC till 2016. In 2006, Professor Affes served as a General Co-Chair of the IEEE VTC'2006-Fall conference, Montreal, Canada. In 2008, he received from the IEEE Vehicular Technology Society the IEEE VTC Chair Recognition Award for exemplary contributions to the success of IEEE VTC. He currently acts as a member of the Editorial Boards of the IEEE TRANSACTIONS ON WIRELESS COMMUNICATIONS, the IEEE TRANSACTIONS ON SIGNAL PROCESSING, the IEEE TRANSACTIONS ON COMMUNICATIONS, and the *Wiley Journal on Wireless Communications & Mobile Computing*.